Agricultural and Forest Meteorology 287 (2020) 107957

Contents lists available at ScienceDirect

Agricultural and Forest Meteorology

journal homepage: www.elsevier.com/locate/agrformet

# Environmental and biophysical controls of evapotranspiration from Seasonally Dry Tropical Forests (*Caatinga*) in the Brazilian Semiarid

Thiago V. Marques[a,b,*], Keila Mendes[a], Pedro Mutti[a], Salomão Medeiros[c], Lindenberg Silva[d], Aldrin M. Perez-Marin[c], Suany Campos[a], Paulo S. Lúcio[a,e], Kellen Lima[a], Jean dos Reis[a], Tarsila M. Ramos[e], Daniel F. da Silva[e], Cristiano P. Oliveira[a,e], Gabriel B. Costa[f], Antonio C.D. Antonino[g], Rômulo S.C. Menezes[g], Cláudio M. Santos e Silva[a,e], Bergson Bezerra[a,e]

[a] Climate Sciences Graduate Program, Federal University of Rio Grande do Norte, UFRN, Natal, Brazil
[b] Federal Institute of Education, Science and Technology of Rio Grande do Norte, IFRN, Natal, Brazil
[c] Institute of Semi-Arid, INSA, Campina Grande, Brazil
[d] Academic Unit of Atmospheric Sciences, Federal University of Campina Grande, UFCG, Campina Grande, Brazil
[e] Department of Atmospheric and Climate Sciences, Federal University of Rio Grande do Norte, UFRN, Natal, Brazil
[f] Institute of Biodiversity and Forests, Federal University of Western Pará, UFOPA, Santarém, Brazil
[g] Department of Nuclear Energy, Federal University of Pernambuco, UFPE, Recife, Brazil

ARTICLE INFO

*Keywords:*
Evapotranspiration
Bulk surface conductance
Decoupling factor
Caatinga Biome
Brazilian Semiarid

ABSTRACT

Seasonally dry tropical forests are among the most important biomes regarding regional and global hydrological and carbon fluxes. Thus, the objective of this study was to evaluate the seasonal and interannual variability of evapotranspiration (*ET*) and its biophysical control and characteristics (surface conductance—$G_s$; decoupling coefficient—Ω; ratio between actual evapotranspiration and equilibrium evapotranspiration—$ET/ET_{eq}$) in a preserved Caatinga Biome environment during two dry years in the Northeast Brazil region. A study on this subject with this level of detail in this biome is unprecedent. Measurements were carried out using an eddy covariance system during the period from 1st January 2014 to 31st December 2015. The lowest *ET* values were observed in the dry season of both experiment years (0.3 and 0.2 mm day$^{-1}$) as a consequence of poor water availability, which favored partial stomatal closure and reduced $G_s$ values (0.22 and 0.13 mm s$^{-1}$). The opposite occurred in the wet season, when *ET* (2.6 and 1.7 mm day$^{-1}$) and $G_s$ (3.74 and 2.13 mm s$^{-1}$) means reached higher values. Regarding annual values, differences between total annual rainfall in both years is the most probable cause for the differences observed in annual *ET* values. In 2014, annual *ET* was of 473.3 mm while in 2015 it was 283.4 mm, which incurred in an overall decrease in $G_s$, Ω and $ET/ET_{eq}$ values. Leaf senescence and extremely low $G_s$ values during the dry season suggest that the trees of the Caatinga Biome are more resilient regarding the use of water and are avoiding water stress caused under low water availability.

## 1. Introduction

The reminiscent areas of Seasonally Dry Tropical Forests (SDTF) are located mostly in the Neotropics and extend from the Northwest of Mexico to the North of Argentina, usually in isolated patches or land segments (Miles et al., 2006; Pennington et al., 2000, 2006; Linares-Palomino et al., 2011). Among the SDTF, the Caatinga Biome located in the Brazilian Semiarid region in the Northeast Brazil is the only one consisted of a fully functional ecosystem which comprises a continuous area of approximately 800,000 km$^2$, representing roughly 10% of the Brazilian territory (Miles et al., 2006; Särkinen et al., 2011; Santos et al., 2012; Koch et al., 2017).

The Caatinga has a variety of endemic species (Sampaio et al., 1995; Leal et al., 2005; Moura et al., 2013) and its vegetation is composed mainly by xerophyte, woody, thorny, deciduous and semi-deciduous physiognomies with a predominance of trees and shrubs morphologically adapted to sustain water stress (Sampaio et al., 1995; Araújo et al., 2007; Mendes et al., 2017). The Brazilian Semiarid region is characterized by low and irregular rainfall, high temperatures and solar radiation, which increase evaporation and soil desiccation, leading to water deficits during most of the year (Dombroski et al., 2011; Mutti et al., 2019), although rainfall extreme events occur throughout

* Corresponding author
*E-mail address:* thiago.valentim@ifrn.edu.br (T.V. Marques).

https://doi.org/10.1016/j.agrformet.2020.107957
Received 15 February 2019; Received in revised form 27 February 2020; Accepted 2 March 2020

the year (Oliveira et al., 2017; Mutti et al., 2019). The Caatinga has been identified as one of the most important wildlife regions of the globe and most biodiverse dry forests (Mittermeier et al., 2003; Pennington et al., 2006; Santos et al., 2014; Koch et al., 2017). Nevertheless, only 1% of this Biome has been converted into protected areas and the Caatinga and other SDTF have received less attention than tropical rainforests regarding research efforts (Koch et al., 2017; Tomasella et al., 2018).

The $CO_2$ transfer rate from the atmosphere to the carboxylation sites during the photosynthesis process is closely related to water lost to the atmosphere through leaf transpiration. These exchanges are controlled by the interaction of various environmental factors (such as solar radiation, air temperature, vapor pressure deficit—*VPD* and soil water content), besides biological processes inherent to the vegetation such as leaf emergence and development and stomatal conductance (Zha et al., 2013). At the plant level, physiological control of $CO_2$ absorption and transpiration is carried out by stomata and the modulation of such processes is quantified in terms of leaf stomatal conductance (Fanourakis et al., 2013; Lin et al., 2015; Wehr et al., 2017). At the ecosystem level, the control of both evapotranspiration (*ET*) and $CO_2$ absorption are quantified in terms of surface conductance ($G_s$) and its relationship with environmental and biological factors.

The quantification of $G_s$ is important not only for understanding the mechanisms that control *ET* and $CO_2$ exchange, but also for calibrating the Penmann-Monteith equation for future applications under the conditions in which $G_s$ was calculated. According to Tan et al. (2019), if there is a viable method to reliably obtain $G_s$ values and its environmental controls, then *ET* can be easily calculated at local and global scales using only usually observed meteorological variables. However, the parameterization of $G_s$ is challenging, since it is regulated by the physical environment but also varies between species, especially in tropical forests (Tan et al., 2019). Usually $G_s$ has been described by the Penman-Monteith equation in its big-leaf version (Tan et al., 2019) and its controls have been analyzed through the relationship between it and different biophysical parameters, such as *VPD*, vegetation indices and the ratio between actual and equilibrium evapotranspiration ($ET/ET_{eq}$). These analyses have been performed in different biomes around the world (Ryu et al., 2008; Zha et al., 2013; Ma et al., 2015; Tan et al., 2019).

Recently, observational studies in the Caatinga have been developed in order to better understand the soil-plant-atmosphere relationship in this biome. It has been observed that the closure of the energy balance is better during the wet season and under very unstable conditions, and most of the net radiation is converted into sensible heat flux (Teixeira et al., 2008; Campos et al., 2019). Mutti et al. (2018) showed that during a wet year, *ET* differences between land cover classes were less noticeable due to soil saturation and the urgency of vegetated surfaces to meet their physiological needs. In a dry year, however, the differences were more evident, with bare soil showing lower *ET* rates and vegetation classes showing higher *ET* values in a Semiarid Brazil watershed predominantly covered by the Caatinga. Da Silva et al. (2017) measured the water and energy fluxes over the Caatinga and found that the *ET* in the dry season was controlled by the vegetation and in the wet season it was controlled by the atmospheric conditions. Studies of this nature are important because they allow a better understanding of the effects of projected climate change scenarios for this biome, which indicate increasing trends in air temperature, higher evapotranspiration rates, decreased rainfall and, consequently, aggravation of water deficit (Magrin et al., 2014; Marengo et al., 2017).

Given the large area of the Caatinga Biome, one can infer that it plays an important role in regional (or even global) processes related to the biosphere-atmosphere interactions (Moura et al., 2016). Previous studies in this biome have clarified some uncertainties about key subjects such as the role of seasonal rainfall on the closure and partitioning of the energy balance, evapotranspiration and $CO_2$ exchange (Teixeira et al., 2008; da Silva et al., 2017; Campos et al., 2019; Mutti et al., 2019; Santos et al., 2020). On the other hand, a detailed analysis of the characteristics of *ET* control in the Caatinga Biome has not yet been developed. Although Teixeira et al., (2008) briefly commented the characteristics of surface resistance (reciprocal of $G_s$), the analysis of environmental controls was not carried out, since it was not the objective of said study. In this sense, more effort is needed in order to better comprehend the environmental and biophysical controls of *ET* and in which way they affect heat and mass transfer in the Caatinga. Thus, long term detailed studies on the energy and water fluxes between vegetation and the atmosphere are needed due to the vulnerability of this environment to anthropic activities and climate change. Furthermore, the accuracy of climate scenarios and their impacts on climate, biodiversity and the population of these region is still debatable, and uncertainties are high (Magrin et al., 2014; Marengo and Bernasconi, 2015). Such a challenge reinforces the critical need for studies on how responds to environmental variables and how it influences energy and mass fluxes, which is particularly important for understanding future biosphere-atmosphere interactions in the Brazilian Semiarid region.

In this context, the objective of this study was to evaluate the seasonal variability of evapotranspiration and its control mechanisms in a preserved Caatinga Biome environment during two dry years. We also analyzed the daytime pattern of evapotranspiration and compared the sensitivity of surface conductance to *VPD*.

## 2. Material and methods

### 2.1. Site description

The study was conducted in a preserved fragment of the Caatinga Biome, in the Rio Grande do Norte State, Brazilian Semiarid. An 11-meters tall flux tower equipped with an eddy covariance system was installed in the Seridó Ecological Station (ESEC-Seridó; 6°34'42"S, 37°15'05"W, 205 m, above sea level), a conservation unit of the Caatinga Biome located between the Serra Negra do Norte and Caicó cities (Fig. 1). The ESEC-Seridó area is managed by the Chico Mendes Institute for Biodiversity Conservation (ICMBio). The flux tower was acquired by the Brazilian National Institute of Semiarid (INSA) and is part of the National Observatory of Water and Carbon Dynamics in the Caatinga Biome (NOWCDCB) network.

The ESEC-Seridó comprises an area of 1163 ha of remnant Caatinga, characterized by a dry and xerophyte forest composed by deciduous and semi-deciduous plant species, predominantly sparsely distributed small trees and shrubs besides herb patches which thrive only during the wet season (Freitas et al., 2010; Souza et al., 2012; Althoff et al., 2016; Tavares-Damasceno et al., 2017). The canopy is around 6 meters high. According to Table 1, which shows the relative frequency (RtF) and the Importance Value (IV) of species which occur in the study area (Santana et al., 2016), one can note that the *Leguminosae* and *Euphorbiaceae* families have the highest count of individuals and there is a balance between the number of tree and shrub species, although the first is dominant (RtF higher than 50%). Shrub species have a RtF of around 23%. Among the four dominant species, three are arboreous (*Caesalpinia pyramidalis* Tul., *Aspidosperma pyrifolium* Mart., and *Anadenanthera colubrina* (Vell.) Brenan) and one is shrub (*Croton blanchetianus* Baill.). Altogether, the three arboreous species have a total RtF higher than 40%.

The region's soil is predominantly Entisol with mainly sandy loam and sandy clay loam textures. It is a shallow (approximately 40 cm) rocky soil, with low fertility and moderately drained (Althoff et al., 2016). The region's climate according to the Köppen's climate classification is Bsh (semiarid low longitude and altitude), with the wet season established between January and May, mean annual rainfall of around 700.0 mm, mean annual temperature of 25.0 °C and mean annual air humidity of around 60% (Alvares et al., 2013;

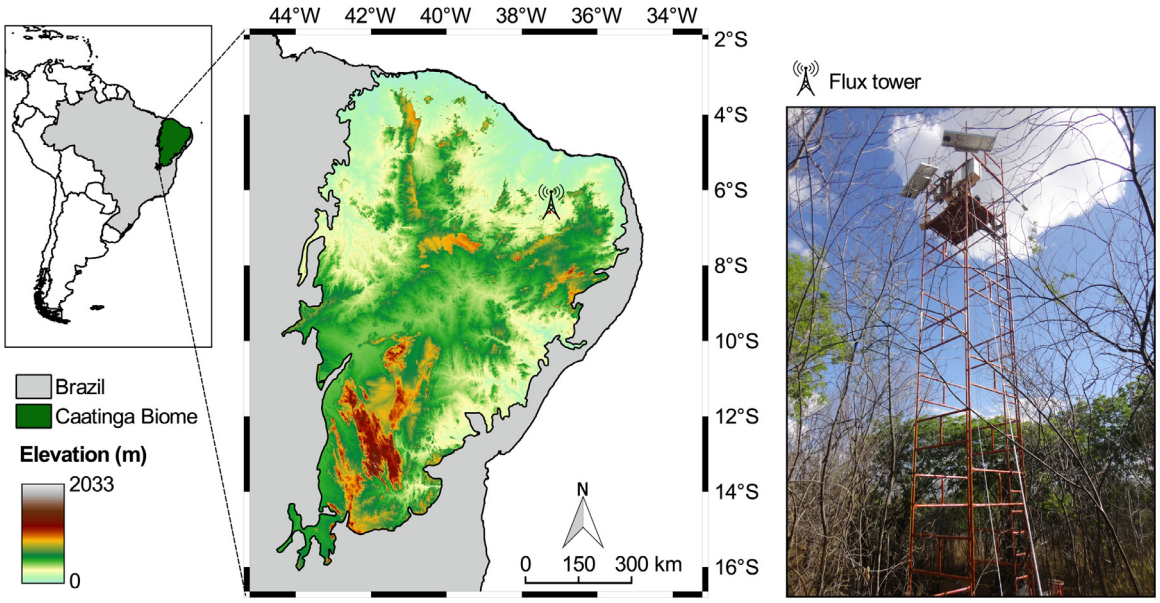


**Fig. 1.** Geographical location of the micrometeorological tower installed in the ESEC-Seridó, Brazil.

Campos et al., 2019). The observation site is mainly flat with slopes varying from 1° to 3° and the distance from the flux tower to the border of the continuous *Caatinga* area is higher than 300 m in the prevailing wind direction.

### 2.2. Measurements and data

The experiment was conducted during two years, from January 2014 until December 2015. Flux tower measurements originated two datasets: i) high frequency data (10 Hz sampling): $CO_2$ and $H_2O_{(v)}$ concentration, the three wind speed components $u_x$, $u_y$ and $u_z$, sonic temperature, high frequency temperature and atmospheric pressure; ii) low frequency data (5s sampling stored as 30 minutes averages): the four components of the radiation balance, air temperature, relative humidity in air, soil heat flux density ($G$). All sensors were installed at an 11.0 m height above the soil (4.0 m above the average vegetation canopy in the region). On the other hand, heat plates for the measurement of $G$ were installed at a 0.05 m depth in the soil. All data were stored in a datalogger model CR3000 (Campbell Scientific, Inc., Logan, UT, USA). A summary of the variables which compose the high frequency and low frequency datasets and their respective measuring instruments is shown in Table 2.

Additionally, we calculate the daily reference evapotranspiration (mm day$^{-1}$) ($ET_0$), which is a variable that depicts the potential water lost from the surface to the atmosphere and was calculated according to the method described in the FAO56 (Allen et al., 1998):

$$ET_0 = \frac{0.408 \cdot \Delta \cdot (Rn - G) + \gamma \cdot \frac{900}{T_a + 273} \cdot u_2 \cdot VPD}{\Delta + \gamma \cdot (1 + 0.34 \cdot u_2)}, \quad (1)$$

where $\Delta$ is the slope of the saturation vapor pressure versus air temperature curve (kPa°C$^{-1}$), $Rn$ is the surface net radiation (MJ m$^{-2}$

**Table 1**
Species, family, common name, life-form, relative frequency (RtF, %) and importance value (IV) sampled in the study area by Santana et al (2016). All scientific names of species were obtained in The Plant List platform*.

| Species | Family | Common name | Life-form | RtF | IV |
|---|---|---|---|---|---|
| *Caesalpinia pyramidalis* Tul. | Leguminosae | Catingueira | Tree | 10.60 | 54.30 |
| *Aspidosperma pyrifolium* Mart. | Apocynaceae | Pereiro | Tree | 11.40 | 51.20 |
| *Croton blanchetianus* Baill. | Euphorbiaceae | Marmeleiro | Shrub | 9.76 | 50.10 |
| *Anadenanthera colubrina* (Vell.) Brenan | Leguminosae | Angico-vermelho | Tree | 10.20 | 20.30 |
| *Mimosa tenuiflora* (Willd.) Poir. | Leguminosae | Jurema-preta | Shrub | 6,91 | 16,96 |
| *Combretum leprosum* Mart. | Combretaceae | Mufumbo | Shrub | 8,13 | 15,83 |
| *Piptadenia stipulacea* (Benth.) Ducke | Leguminosae | Jurema-branca | Shrub | 6.10 | 14.40 |
| *Commiphora leptophloeos* (Mart.) J.B.Gillett | Burseraceae | Umburana | Tree | 6.10 | 13.70 |
| *Jatropha mollissima* (Pohl) Baill. | Euphorbiaceae | Pinhão bravo | Shrub | 2.60 | 13.40 |
| *Erythroxylum pungens* O. E. Schulz | Erythroxylaceae | Rompe-gibão | Shrub | 6,50 | 12,20 |
| *Caesalpinia ferrea* C. Mart. | Leguminosae | Jucá | Tree | 2.03 | 8.150 |
| *Croton heliotrophiilious* Kunth | Euphorbiaceae | Velame | Herbaceous | 6.77 | 3.66 |
| *Handroanthus impetiginosus* (Mart. ex DC.) Mattos | Bignoniaceae | Ipê roxo | Tree | 5.37 | 3.66 |
| *Cnidoscolus quercifolius* Pohl | Euphorbiaceae | Faveleira | Tree | 3.71 | 2.03 |
| *Bignonia corymbosa* (Vent.) L.G.Lohmann | Bignoniaceae | Bugi | Liana | 3.17 | 2.03 |
| *Bauhinia cheilantha* (Bong.) Steud. | Leguminosae | Mororó | Shrub | 2.97 | 1.22 |
| *Amburana cearensis* (Allemao) A.C.Sm. | Leguminosae | Cumaru | Tree | 0.81 | 1.90 |
| *Senna macranthera var. micans* (Nees) H.S.Irwin & Barneby | Leguminosae | Canafístula | Shrub | 0.81 | 1.35 |
| *Chamaecrista hispidula* (Vahl) H.S.Irwin & Barneby | Leguminosae | Maria-preta | Shrub | 0.81 | 1.01 |
| *Cereus jamacaru* DC. | Cactaceae | Mandacaru | Tree | 0.41 | 0.62 |
| *Cynophalla flexuosa* (L.) J.Presl | Capparaceae | Feijão-bravo | Shrub | 0.41 | 0.49 |
| *Lantana camara* L. | Verbenaceae | Chumbinho | Herbaceous | 0.41 | 0.46 |

* Available on http://www.theplantlist.org/. Accessed in Oct 12, 2018.

**Table 2**
Measured variables, description of the instruments installed in the flux tower of the preserved Caatinga area in the Seridó Ecological Station, Rio Grande do Norte, Brazil, and their sampling frequency.

| Variable | Instrument (Manufacturer) | Sampling |
|---|---|---|
| $CO_2$ and $H_2O$ concentrations | $CO_2$/$H_2O$ Open-Path Gas Analyzer EC150 (Campbell Scientific, Inc., Logan, UT, USA) | 10 Hz |
| $u_x$, $u_y$, $u_z$, sonic temperature | 3D Sonic Anemometer model CSAT3 (Campbell Scientific, Inc., Logan, UT, USA) | 10 Hz |
| Atmospheric pressure (hPa) | *Enhanced Barometer model PTB110 (*Vaisala Corporation, Helsink, Finland). | 10 Hz |
| High frequency temperature (°C) | HMP155A probe (Vaisala Corporation, Helsinki, Finland) | 10 Hz |
| Net radiation components | CNR4 net radiometer (Kipp & Zonen BV, Delft, The Netherlands) | 5 s |
| Air temperature (°C) and relative humidity (%) | Temperature and Relative Humidity Probe model HMP45C (Vaisala Corporation, Helsink, Finland) | 5 s |
| Soil heat flux (W/m$^2$) | Soil heat Flux Plates model HFP01SC (Hukseflux Thermal Sensors, Delft, The Netherlands) | 5 s |

day$^{-1}$), $G$ is the soil heat flux (MJ m$^{-2}$ day$^{-1}$), γ is the psychrometric constant (kPa°C$^{-1}$), $T_a$ is the mean air temperature (°C), $u_2$ is the wind speed at 2 m height (m s$^{-1}$), and *VPD* is the vapor pressure deficit (kPa) or the difference between the saturation pressure ($e_s$) and partial pressure ($e_a$). The methods used to calculate Δ, *Rn, G,* γ, $u_2$, $e_s$ and $e_a$ are described in detail by Allen et al. (1998).

### 2.3. Data processing

The energy balance (EB) equation depicts the conversion of net energy in energy and mass fluxes between the canopy and the atmosphere. Neglecting the energy stored in the canopy and the energy used by plants in the photosynthesis and respiration processes, which represent less than 2% of total net radiation (Heilman et al., 1994; Allen et al., 1998), the EB equation can be written as:

$$Rn = H + \lambda E + G, \quad (2)$$

where λ$E$ and $H$ are the latent and sensible heat flux densities, respectively. All components of the previous equation were analyzed as half-hourly averages in W m$^{-2}$.

Sensible and latent heat turbulent fluxes were determined using high frequency data measured by the eddy covariance system based on the equations:

$$H = \rho_{air} \cdot c_p \cdot \overline{w'T'} \text{ and} \quad (3)$$

$$\lambda E = \rho_{air} \cdot \lambda \cdot \overline{w'q'}, \quad (4)$$

where $\rho_{air}$ is the air density (1.2 kg m$^{-3}$), λ is the latent heat of water vaporization (2.45 × 10$^6$ J kg$^{-1}$), $w'$ is the deviation from the mean of vertical wind velocity field (m s$^{-1}$), $q'$ is the deviation from the mean of specific humidity (kg of water/kg of air), $c_p$ is the specific heat of moist air at constant pressure (1004 J kg$^{-1}$ °C$^{-1}$) and $T'$ is the deviation from the mean of air temperature (K).

In order to obtain half-hourly average fluxes, 10 Hz raw data were processed in the EdiRe software (Rob Clement, University of Edinburgh, Scotland). Raw data in the TOB3 (table-oriented-binary 3) binary format was read and converted into TOB1 (table-oriented-binary 1) using the LoggerNet 4.3 software (Campbell Scientific, Inc., Logan, UT, USA) in order to allow data processing. The output data file consisted of a spreadsheet with the turbulent variables used in this study indexed as 48 half-hourly data per day.

The procedures carried out for the processing of data have been thoroughly described in Campos et al. (2019), which used the same dataset of the present study. Data processing included the detection of spikes, delay correction of $H_2O$ / $CO_2$ in relation to vertical wind component, coordinates correction (2D rotation) using planar fit method, correction of spectral loss, sonic virtual temperature correction, corrections for flux density fluctuations (Webb et al., 1980), as well as the incorporated frequency response correction derived from Moore (1986) and Massman (2000). We also applied corrections regarding the reduction of wind velocity or the increase in turbulence caused by the shadow of the tower and the sensor. As the sensor was installed in order to remain pointed towards the predominant wind direction according to the equipment user guide (Campbell Scientific Inc., 2012), there were few data in the shadow zone direction.

Physically inconsistent values (spikes) caused by changes in the footprint or imprecise measurements were identified as sudden gaps in the time series of the 30 minutes energy fluxes averages. For the identification of other spikes, we used an algorithm based on the comparison between the difference of each half-hourly value and the range of the moving median daily cycle, as described by Papale et al. (2006). Regarding data quality, only high and medium quality data were analyzed (flags 1 and 2), while low quality data (flag 3) were discarded.

In this experiment there were two main situations where data were lacking: i) data gaps caused by spikes identification and removal, but no gaps in the meteorological dataset; ii) data gaps both in the flux measurements and in the meteorological dataset. Turbulent fluxes data gaps were filled using the method described by Reichstein et al. (2005) where the friction velocity ($u_*$) filtering was estimated according to the method described by Papale et al. (2006) with the aid of the online platform developed by the Max Planck Institute for Biogeochemistry (http://www.bgc-jena.mpg.de/~MDIwork/eddyproc/).

### 2.6. Footprint calculation

The flux footprint was calculated using the two-dimensional parameterization model called Flux Footprint Prediction, as described by Kljun et al. (2015). This model requires the following data: flux measurement height ($z_m = 11\ m$), zero-plane displacement ($d$), surface friction velocity ($u_*$), vertical wind velocity deviation ($\sigma_w$) and roughness length ($z_0$). In our study site the canopy height ($h$) was of 6 m. However, this parameterization is valid for moderate friction velocity values ($u_* > 0.1\ m\ s^{-1}$) and for a limited range of boundary layer stability conditions ($-15.5 \leq z_m/L$), where $L$ is the Monin-Obukhov length (Kljun et al. (2015). In our study area, Campos et al. (2019) previously considered $d = (2/3) \cdot h$ and $z_0 = 0.123 \cdot h$.

### 2.7. Bulk surface parameters

The ability of a given surface to transfer water vapor to the atmosphere is what defines $G_s$. Obtaining $G_s$ and aerodynamic conductance ($G_a$) is crucial to understand the dynamics and mechanisms involved in mass exchange (*ET* and $CO_2$) between terrestrial ecosystems and the atmosphere, as reported by Rocha et al. (2004), Zha et al. (2013), and Ma et al. (2015). $G_s$ values in the Caatinga Biome were calculated through the inverted Penman–Monteith equation (Stewart, 1988):

$$G_s = \frac{G_a \cdot \gamma \cdot \lambda E}{\Delta \cdot (Rn - G) + \rho_{air} \cdot c_p \cdot G_a \cdot VPD - \lambda E \cdot (\Delta + \gamma)}. \quad (5)$$

In the present study, the final values of $G_s$ were transformed from m s$^{-1}$ to mm s$^{-1}$ to agree with other studies. The term $G_a$ is the aerodynamic conductance which is reciprocal to the aerodynamic resistance to water vapor transport ($r_a$), which in turn varies according to surface roughness and wind speed. The $r_a$ parameter comprises the aerodynamic resistance for momentum ($r_{aM}$) and the quasi-laminar

layer resistance ($r_b$), connected in series according to the following equation (Thom, 1972; Tan et al., 2019):

$$G_a = G_{aM} + G_b \quad \text{or} \quad \frac{1}{r_a} = \frac{1}{r_{aM}} + \frac{1}{r_b}. \tag{6}$$

From $\tau = \rho u_*^2 = \rho u G_{aM}$, where $\tau$ is the vertical flux of horizontal momentum, some previous studies such as Szeicz et al. (1969), have shown that:

$$G_{aM} = u_*^2/u \quad \text{or} \quad r_{aM} = u/u_*^2, \tag{7}$$

where $u$ is the wind speed measured at a height $z$, and $u_*$ is the friction velocity, both measured in m $s^{-1}$. According to Tan et al. (2019), Eq. (7) provides the best and most reliable $G_{aM}$ estimates over tropical forests.

According to Monteith and Unsworth (2013) the values of $r_b$ are rarely determined directly. However, they can be estimated from values of parameters observed in field experiments. Also according to Monteith and Unsworth (2013), Thom's empirical equation (Eq. (8)) is an adequate approximation of $r_b$, at least for $u_*$ values typically in the range between 0.1 and 0.5 m $s^{-1}$, which is the case of observational values in our experimental site (Campos et al., 2019):

$$r_b = 6.2 \cdot u_*^{-0.67}. \tag{8}$$

By combining Eqs. (6)–(8) we get the equation for $G_a$:

$$G_a = \left( \frac{u}{(u_*)^2} + 6.2 \cdot (u_*)^{-0.67} \right)^{-1}, \tag{9}$$

where $u$ is the wind speed above the canopy measured by the sonic anemometer.

The degree of the surface-atmosphere interaction was evaluated using the decoupling coefficient, which is dimensionless, and was used to describe the sensitivity of evapotranspiration to shifts in surface conductance according to the following equation (Jarvis and McNaughton, 1986):

$$\Omega = \frac{\Delta/\gamma + 1}{\Delta/\gamma + 1 + G_a/G_s}, \tag{10}$$

where Ω ranges from 0 to 1. According to Baldocchi and Xu (2007) and Ma et al. (2015), when $\Omega \to 1$ the surface is completely decoupled from overhead conditions. In this case, ET is mainly controlled by available energy. On the other hand, when $\Omega \to 0$, ET is mainly controlled by bulk surface conductance, indicating a strong influence of the vegetation in the control of ET and the atmospheric humidity deficit.

In order to determine whether atmospheric demand or surface moisture supply was the limiting factor, we calculated the ratio between $ET$ and equilibrium evapotranspiration ($ET_{eq}$). The daytime mean (08:00–17:00 local time) was obtained through an adapted version of the $\lambda E_{eq}$ equation proposed by Priestley and Taylor (1972):

$$\frac{ET}{ET_{eq}} = \frac{\Delta + \gamma}{\Delta} \cdot \frac{\lambda E}{H + \lambda E}. \tag{11}$$

Using the $ET/ET_{eq}$ ratio to compare different observational sites is reasonable since they are normalized by the equilibrium rates mainly determined by $Rn$ (Wilson and Baldocchi, 2000).

### 2.8. Vegetation condition

In order to assess the behavior of the vegetation during the experiment we used remote sensing data obtained through the Moderate Resolution Imaging Spectroradiometer (MODIS) sensor aboard the Terra and Aqua satellites and made available by the United States Geological Survey (USGS) (https://earthexplorer.usgs.gov). We used both Normalized Difference Vegetation Index (NDVI) and Leaf Area Index (LAI) data. The NDVI was retrieved from the MOD13A2 (v006)—Terra Vegetation Indices product, which provides vegetation indices data as 16-day composites by selecting the best values in this period according to clear sky conditions and the imaging angle (Didan, 2015). For the LAI we used the MCD15A3H (v006)—Terra + Aqua LAI product, which consists of 4-day composites by selecting the best values in the period from both satellites (Myneni et al., 2015).

### 2.9. Statistical analysis

The daily means and totals of the meteorological variables, fluxes and ET control mechanisms were bootstrapped over seasonal intervals for the estimation of random variance ( ± 95% of confidence interval – CI) about the mean according to the methodology presented by Zanella de Arruda et al. (2016). Statistically significant differences ($p < 0.05$) in the mean seasonal value for a given meteorological variable, flux or ET control mechanism were determined by the degree of overlap in the 95% bootstrapped CI (Zanella de Arruda et al., 2016). Linear and non-linear regression models were used to evaluate the relationship between two given variables. Additionally, the model coefficients were tested under the null hypothesis at a 5% significance level. All statistical analysis was carried out using the R software (R Core Team, 2018).

## 3. Results

### 3.1. Seasonal analysis

Seasonal analysis was carried out considering the behavior of daily accumulated rainfall during the experiment. Thus, the following seasons were defined: i) wet season, from February to May in 2014 (419.6 mm) and from February to April in 2015 (381.5 mm); ii) dry season, from August to October in 2014 (6.2 mm) and from August to November in 2015 (0.0 mm); iii) wet-dry transition season, from June to July in 2014 (21.6 mm) and from May to July in 2015 (56.0 mm); and iv) dry-wet transition season, in the months of January and December in 2014 and 2015 (65.6 mm and 28.5 mm, respectively).

### 3.2. Weather conditions

Annual rainfall in 2014 and 2015 was of 513 mm and 466 mm, respectively while the 30-year average in the region is of 758 mm. Daily rainfall rates in 2014 and 2015, as shown in Fig. 2a, highlight the marked rainfall seasonal variability in the study area. In the course of the experiment years, roughly 82% of total rainfall was registered during the wet season (Table 3) and in 2014 rainfall was more homogeneously distributed, with 71 rain days (Fig. 2a) and a daily maximum of 45.4 mm. In 2015, on the other hand, only 34 rain days were registered (Fig 2a.) with two events (65 mm and 60 mm) above the heavy rainfall events threshold, which is of 50 mm in the study area (Oliveira et al., 2017).

Besides rainfall, Fig. 2a also shows daily $ET_0$ values, which were predominantly above 6 mm with a daily average of 8.0 mm $day^{-1}$ in 2014 and 8.3 mm $day^{-1}$ in 2015 ($p < 0.05$; Table 3). Fig 2b–d shows daily global radiation ($R_g$ in MJ $m^{-2}$), $T_a$, soil temperature ($T_s$ in °C) and $VPD$ values, respectively, in which a clear seasonal variation can be observed. In 2014, mean $R_g$ was of 22.0 MJ $m^{-2}$ $day^{-1}$ (Table 3), ranging from 11.4 to 27.6 MJ $m^{-2}$ $day^{-1}$ with maximum values occurring mainly during the dry-wet transition season, while minimum values were observed in the wet-dry transition season. In 2015, $R_g$ had the same pattern observed in 2014, with maximum and minimum values observed in the same periods and a mean value of 22.6 MJ $m^{-2}$ $day^{-1}$ ranging from 11.0 to 27.5 MJ $m^{-2}$ $day^{-1}$ (Table 3 and Fig. 2b).

The seasonality of $T_a$ (and $T_s$) was consistent with $R_g$, with a mean value of 28.9 °C (31.4 °C) in 2014 (Table 3) ranging from 24.7 °C (27.4 °C) in the wet season to 32.2 °C (37.0 °C) in the dry-wet season (Fig. 2c), while in 2015 the mean value was of 29.5 °C (32.9 °C), ranging from 25.5 °C (27.3 °C) in the wet-dry season to 32.4 °C (38.5 °C) in

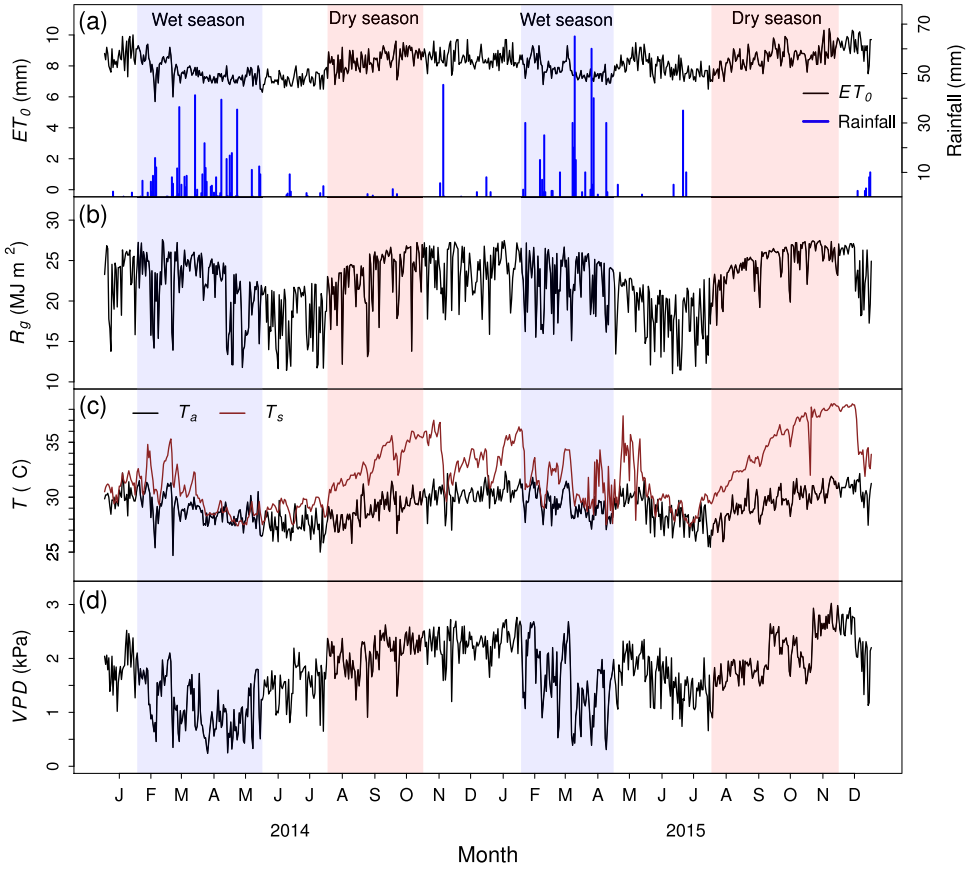


**Fig. 2.** Accumulated rainfall and daily means for (a) reference evapotranspiration ($ET_0$), (b) global incident radiation ($R_g$), (c) air and soil temperature ($T_a$ and $T_s$) and (d) vapor pressure deficit (*VPD*) during the studied period in the Caatinga (ESEC-Seridó). Blue and red shades represent wet and dry periods, respectively.

the dry-wet season (Table 3 and Fig. 2c). The *VPD* mean value was 1.7 kPa in 2014 and 1.9 kPa in 2015 (Table 3). The highest daily *VPD* means were registered in the dry season of 2014 (2.7 kPa) and 2015 (3.0 kPa) while the minimum means (0.2 kPa and 0.3 kPa) were registered in the wet seasons of 2014 and 2015 (Table 3 and Fig. 2d). Overall, the variables presented higher annual means if compared to the 30-year average (21.6 MJ m$^{-2}$ day$^{-1}$, 26.8 °C and 1.3 kPa, respectively for $R_g$, $T_a$ and *VPD*).

### 3.3. Footprint and wind direction

The footprint calculated from the location of the eddy covariance tower ranged from 150 meters (wet season) to 200 meters (dry season). One should notice that the distance from the eddy covariance tower to the border of the conservation unit is larger than 300 m, so the footprint calculated is adequate for this study (Campos et al., 2019). The predominant local wind direction during the study period was southeast (Fig. 3) due to the influence of the South Atlantic Subtropical High as reported by previous studies on the climatology of the region (Santos and Santos e Silva, 2013; Gilliland and Klein, 2018).

### 3.4. Diurnal and seasonal changes

Fig. 4 shows the mean diurnal cycle of *ET* and its controlling factors ($G_s$ and Ω) in 2014 (left panel) and 2015 (right panel). According to Fig. 4a and b, $G_s$ increased sharply from sunrise (06:00 local time) until it reached its maximum values between 08:00 and 10:00 local time. From this time on, $G_s$ values decreased almost linearly until they've become stationary during the night (0.01 mm s$^{-1}$) in both years and in all seasons, except during the dry season when its values were almost constant during daytime. The diurnal pattern of *ET* (Fig. 4c–d) was relatively consistent with the $G_s$ curve but with higher values between 10:00 and 14:00 local time.

One can notice in Fig. 4e–f that the behavior of the diurnal cycle of Ω was similar during all seasons and in both years; after sunrise (about 06:00 local time) there was a sharp increase until it reached its

**Table 3**
Daily mean ± standard deviation for global radiation ($R_g$, MJ m$^{-2}$ day$^{-1}$), vapor pressure deficit (*VPD*, kPa), air temperature ($T_a$, °C), soil temperature ($T_s$, °C), and reference evapotranspiration ($ET_0$, mm); seasonal and annual rainfall (Rainfall, mm) and reference evapotranspiration (Total $ET_0$, mm) totals.

| Variable | Dry-wet transition | | Wet season | | Wet-dry transition | | Dry season | | Anual | |
|---|---|---|---|---|---|---|---|---|---|---|
| | 2014 | 2015 | 2014 | 2015 | 2014 | 2015 | 2014 | 2015 | 2014 | 2015 |
| $R_g$ | 23.5 ± 3.1 | 24.3 ± 2.9 | 22.0 ± 3.8 | 22.5 ± 3.2 | 18.0 ± 3.4 | 18.5 ± 3.3 | 23.0 ± 3.3 | 24.8 ± 2.2 | 22.0 ± 3.9 | 22.6 ± 3.8 |
| *VPD* | 2.1 ± 0.4 | 2.3 ± 0.4 | 1.1 ± 0.5 | 1.6 ± 0.6 | 1.5 ± 0.3 | 1.6 ± 0.4 | 2.1 ± 0.3 | 2.1 ± 0.4 | 1.7 ± 0.6 | 1.9 ± 0.6 |
| $T_a$ | 30.1 ± 0.9 | 30.6 ± 0.8 | 28.8 ± 1.3 | 29.3 ± 1.1 | 27.5 ± 1.0 | 28.6 ± 1.4 | 28.9 ± 1.1 | 29.6 ± 1.3 | 28.9 ± 1.4 | 29.5 ± 1.4 |
| $T_s$ | 32.8 ± 1.9 | 35.1 ± 2.3 | 30.1 ± 2.0 | 31.4 ± 1.9 | 29.0 ± 0.7 | 30.3 ± 2.2 | 33.2 ± 1.7 | 34.8 ± 2.7 | 31.4 ± 2.4 | 32.9 ± 3.1 |
| Rainfall | 65.6 | 28.5 | 419.6 | 381.5 | 21.6 | 56.0 | 6.2 | 0.0 | 513.0 | 466.0 |
| $ET_0$ | 8.6 ± 0.6 | 8.9 ± 0.7 | 7.6 ± 0.7 | 7.8 ± 0.6 | 7.2 ± 0.4 | 7.9 ± 0.6 | 8.4 ± 0.6 | 8.6 ± 0.7 | 8.0 ± 0.8 | 8.3 ± 0.8 |
| Total $ET_0$ | 788.1 | 551.6 | 910.8 | 689.8 | 438.6 | 730.2 | 771.6 | 1043.7 | 2909.1 | 3015.3 |

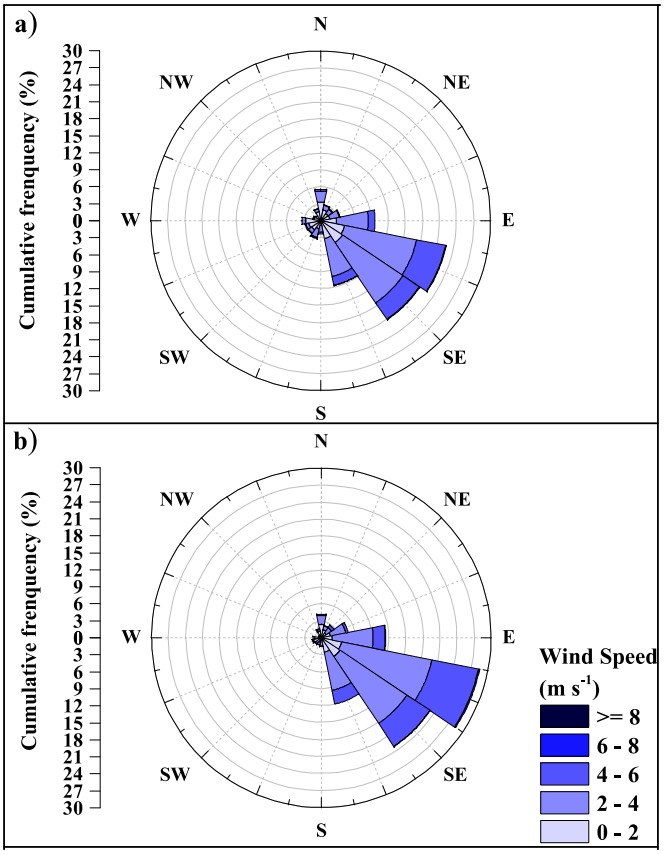


**Fig. 3.** Wind direction and cumulative frequency during the experiment years in the study area. Colors represent wind speed classes.

maximum daily values around 08:00–9:00 local time. From this time on, it decreased almost linearly until sunset (about 18:00 local time) and it remained fairly constant during the night. The highest daily variability was observed during the wet season, from 0.1 to almost 0.4 in 2014 and from 0.1 to 0.3 in 2015. In the transition seasons the maximum daily value was slightly larger than 0.1 and during the dry season Ω was almost constant and close to 0.0, indicating a situation of permanent decoupling or water deficit.

By observing the whole experimental period, one can notice clear seasonal variations in NDVI, $G_s$, $ET$, $ET/ET_{eq}$ and Ω daily values (Fig. 5). Changes in the Caatinga phenology were evaluated using the LAI and NDVI (Fig. 5a). In the wet season, LAI (NDVI) peaked at 3.3 $m^2m^{-2}$ (0.76) in 2014 and 2.5 $m^2m^{-2}$ (0.73) in 2015, gradually decreasing in response to water deficit and the senescence of vegetation, which is composed by deciduous and semi-deciduous plant species. Results show that in the dry season the mean LAI decreased as much as 73% in 2014 and 57% in 2015 (Table 4). Considering annual means, both the LAI and NDVI were higher in 2014 (1.26 $m^2m^{-2}$ and 0.49) than in 2015 (1.02 $m^2m^{-2}$ and 0.44) (Table 4).

The seasonal patterns of $G_s$ daily means are shown in Fig. 5b. The lowest $G_s$ values were found during the dry season with 95% of them below 0.4 mm $s^{-1}$. In the wet-dry transition season $G_s$ values gradually decreased as the environment became drier while the opposite was observed during the dry-wet transition season. The $G_s$ parameter was higher in the wet season, when the LAI reached its maximum values. Thus, increased rainfall and soil moisture contributed to higher $G_s$ values, which peaked at 8.65 mm $s^{-1}$ in 2014 and 7.30 mm $s^{-1}$ in 2015 (Fig. 5b). In 2014, $G_s$ values were 52% (wet season) and 23% (dry season) higher than in 2015.

ET fluxes (Fig. 5c) presented a seasonal variation similar to that of the NDVI and $G_s$ because of the seasonal behavior of leaf physiology and the effect of the forest floor $ET$ in periods of leaf loss. As expected, maximum evapotranspiration rates were registered during the wet season, while minimum rates were observed during the dry season. Peak evapotranspiration in the wet season in 2014 (4.35 mm $day^{-1}$) was higher than in 2015 (3.82 mm $day^{-1}$). On the other hand, most $ET$ values during the dry season were < 0.1 mm $day^{-1}$ in 2014 and > 0.5 mm $day^{-1}$ in 2015. Annual accumulated $ET$ during 2014 was of 473.3 mm while in 2015 it was 283.4 mm (Table 4). The $ET/ET_{eq}$ ratio mean value was of 0.39 ranging from 0.01 to 1.26 in 2014 and of 0.24 ranging from 0.01 to 1.07 in 2015. Regarding seasonal variability, the highest and lowest $ET/ET_{eq}$ values were observed, respectively, in the wet and dry seasons in both years. $ET/ET_{eq} > 1$ probably occurred due to moisture advection during the wet season towards the continent (tower flux site), associated with the confluence of northeasterly and southeasterly trade winds which are part of the Intertropical Convergence Zone (ITCZ). This confluence is highly associated with the southernmost positioning of the ITCZ during this period, which modulates the wet season over the region (Hastenrath, 2006).

The decoupling coefficient (Ω) was calculated in order to determine the relative importance of $G_s$ to changes in annual, seasonal and daily evapotranspiration rates. In the dry and transition seasons, Ω diurnal cycle values were below 0.1 with minimums during the night, suggesting a greater stomatal control in water loss by plants throughout the day (Fig. 4e–f). Estimates of Ω ranged from 0.01 (dry season) to 0.54 (wet season) with a 0.14 mean in 2014 and from 0.01 (dry season) to 0.48 (wet season) with a 0.07 mean in 2015. Thus, as expected, higher Ω values were registered during the wet season while lower values were observed during the dry season (Fig. 4c and Table 4), indicating that surface conductance increasingly controlled $ET$ with the persistence of dry conditions.

### 3.5. Physiological control via surface conductance

The ratio between actual evapotranspiration and equilibrium evapotranspiration ($ET/ET_{eq}$) and $G_s$ in each season of 2014 and 2015 in the Caatinga are shown in Fig. 6. It is possible to observe that there is a non-linear relationship between $ET/ET_{eq}$ and $G_s$, with the highest values during the wet season. The equilibrium $ET/ET_{eq} \approx 1$ is reached when $G_s \approx 8$ mms$^{-1}$, which happens only occasionally in both years, but with less frequency during 2015, which was a drier year.

Overall, $G_s$ decreases exponentially with the increase in $VPD$ (Fig. 7). In the dry season, a $VPD > 1.5$ kPa resulted in close to zero $G_s$ values. However, the effects of $VPD$ on $G_s$ were clearer in 2014 than in 2015 ($R^2 = 0.63$ and 0.19, respectively). Fig. 8 shows the relationship between $G_s$ (08:00–17:00 local time) and the NDVI and LAI. In 2014, $G_s$ increased exponentially with the increase in the NDVI ($R^2 = 0.97$; $p < 0.01$) while in 2015 the relationship was weaker ($R^2 = 0.52$; $p < 0.05$) and could be represented by a first degree polynomial (Fig. 8a–b). Regarding the LAI, its relationship with $G_s$ in 2014 is also exponential ($R^2 = 0.52$; $p < 0.01$) while in 2015 it can be represented by a first degree polynomial ($R^2 = 0.32$; $p < 0.05$) (Fig. 8c–d). Table 5 shows rainfall, total evapotranspiration, daily mean $\lambda E$, mean surface conductance, daily mean Ω and $ET/ET_{eq}$ ratio observed in our study and in different ecosystems with similar climate characteristics.

## 4. Discussion

### 4.1. Meteorological aspects

The annual analysis of the $VPD$ was consistent when comparing the results of 2014 and 2015, that is, the year with less rainfall volume (2015) was warmer and drier, which resulted in higher $VPD$ values. Seasonal variations were also similar to the values reported in Brazilian tropical savannas (Rodrigues et al., 2014) and deciduous tropical forests in northern Thailand (Igarash et al., 2015), which also present vegetation susceptible to extended drought periods. On the other hand,

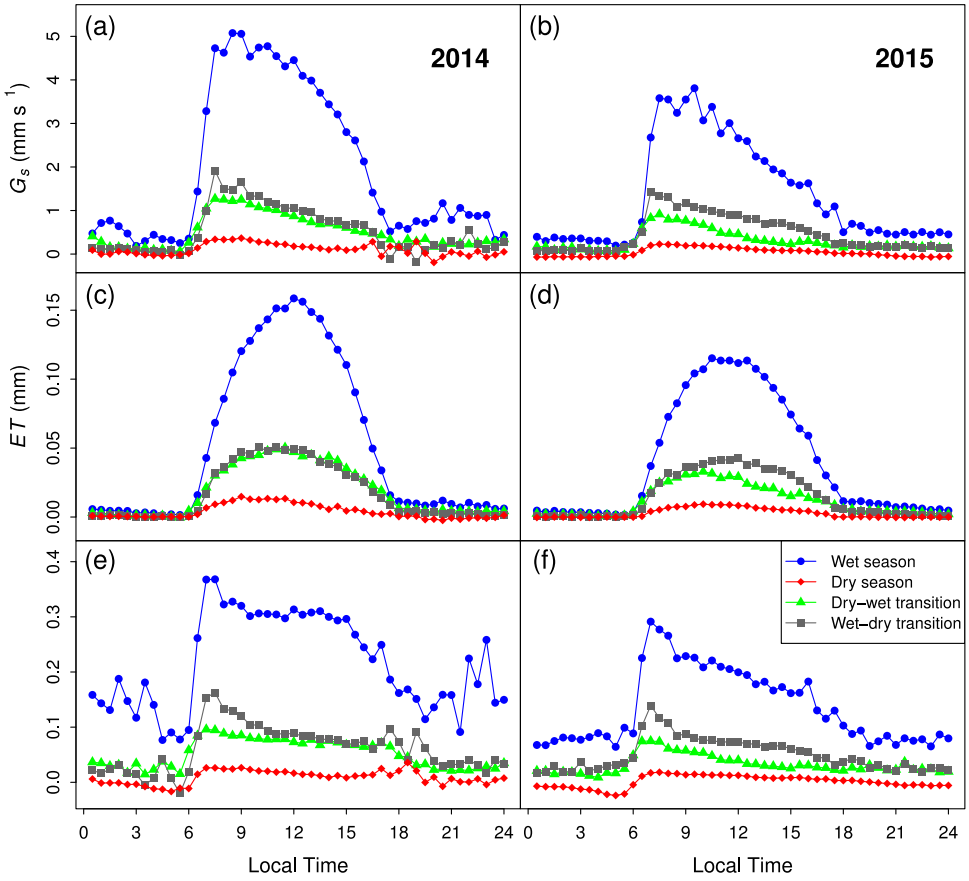


**Fig. 4.** Diurnal variations in evapotranspiration (*ET*), surface conductance ($G_s$) and decoupling coefficient (Ω) by season during the study period in the Caatinga (ESEC-Seridó).

*VPD* values found in this study were higher than the ones found in tropical forest-transitions (Vourlitis et al., 2008) and tropical rainforests (da Rocha et al., 2004), because in these biomes annual rainfall can reach up to 2,000 mm and the seasonal variability of relative humidity in air is not significant. Values presented in Table 3 were also higher than the ones reported by da Silva et al. (2017) during the 2014–2015 drought period, but in a Caatinga region with different characteristics from the present study, which may influence evapotranspiration rates and therefore relative humidity in air.

Daily mean $ET_0$ values greater than 6 mm (Fig. 2a) are consistent with other databases over the region (such as Xavier et al., 2015, for example) and highlights the high atmospheric demand for water in the studied region. Annual mean values of 8.0 mm day$^{-1}$ in 2014 and 8.3 mm day$^{-1}$ in 2015 ($p < 0.05$; Table 3) also reaffirm a more intense drought in 2015 than in 2014.

### 4.2. Diurnal and seasonal changes

LAI was strongly influenced by rainfall distribution and, consequently, soil moisture conditions during the experiment period, which is crucial to leaf coverage seasonality in the Caatinga. The marked seasonality of rainfall and soil moisture in the Caatinga affects phenology, stomatal conductance seasonality and photosynthesis (Santos et al., 2012; Mendes et al., 2017). The study by Mutti et al. (2019) reports that the phenological response of the Caatinga (in the same study site), or its vegetation dynamic, is closely related to rainfall seasonality, which modulates the physiological and metabolic characteristics, and the LAI of plants in this region. Furthermore, Mendes et al. (2017) showed that *C. blanchetianus* populations, an endemic semi-deciduous species, have high adaptive capacity to environmental changes, mainly due to the stomatal closure. Additionally, the authors of said study also reported that the morpho-physiological response of the *C. blanchetianus* is modulated mainly by water availability.

The pattern of the diurnal cycle of $G_s$ was consistent in each studied year and season, but the range between maximum and minimum half-hourly values was higher in the wet season (Fig. 4a–b). The higher $G_s$ values found during the morning agree with other studies that observed maximum surface and canopy conductance between 8:00 and 12:00 and minimum values during sunset in different environments such as tropical Brazilian savannas (Giambelluca et al., 2009; Rodrigues et al. 2014, 2016) and tropical semi-deciduous forest in the southern Amazon Basin (Vourlitis et al., 2008). Furthermore, the Spearman's correlation coefficient (ρ) indicated a decrease in $G_s$ after noon which may be explained by the increase in air temperature ($\rho = -0.67$ and $-0.59$ in the wet season of 2014 and 2015, respectively; $\rho = -0.28$ and $-0.37$ in the dry season of 2014 and 2015, respectively), decrease in relative humidity of air ($\rho = 0.55$ and 0.62 in the wet season of 2014 and 2015, respectively; $\rho = 0.45$ and 0.25 in the dry season of 2014 and 2015, respectively) and higher *VPD* ($\rho = -0.51$ and $-0.62$ in the wet season of 2014 and 2015, respectively; $\rho = -0.40$ and $-0.32$ in the dry season of 2014 and 2015, respectively). Stomatal closure during the higher evaporative demand periods is a mechanism of adjustment to stress conditions in order to maintain plant available water (Flexas et al., 2004; Pinho-Pessoa et al., 2018). There are a number of plant-scale studies on the stomatal closure of Caatinga tree species when leaves are exposed to high *VPD* at low water availability conditions (Santos et al., 2014; Mendes et al., 2017; Pinho-Pessoa et al., 2018). Such studies reported that stomatal conductance varied during the diurnal cycle at ambient temperature and humidity, with higher values between 8:00 and 11:00.

In the present study, seasonal increases and decreases in $G_s$ were

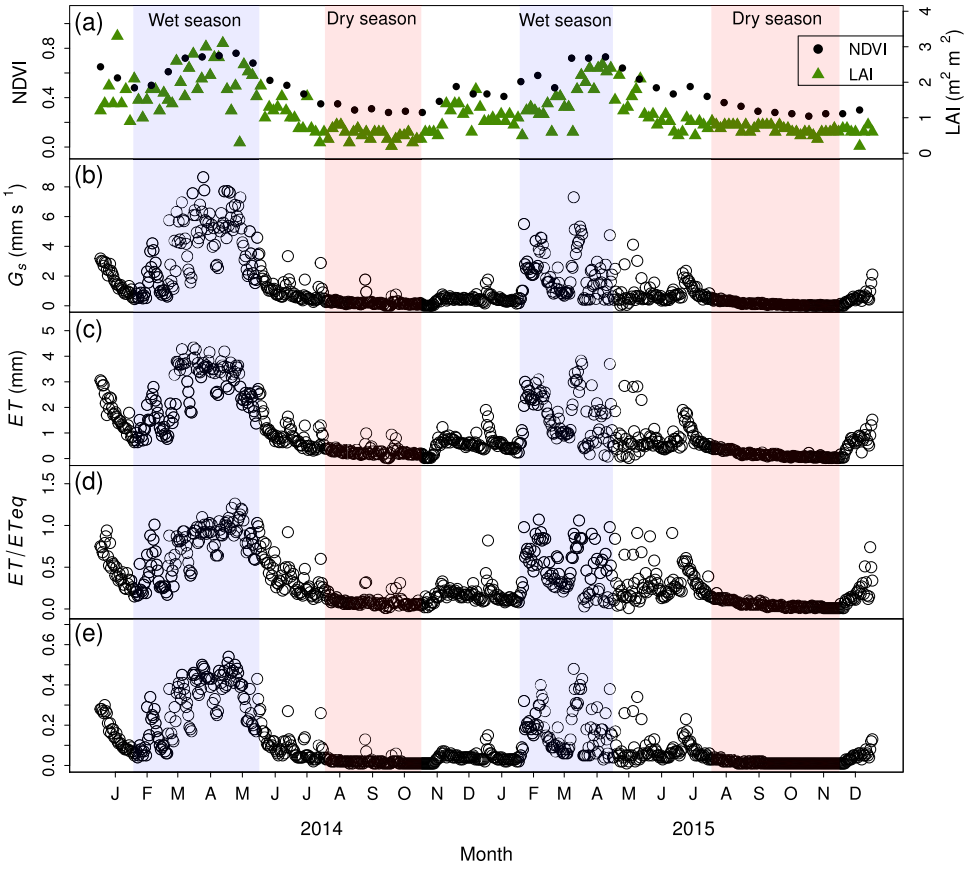


**Fig. 5.** (a) Leaf area index (LAI) and NDVI; daily means (08:00–17:00 local time) for (b) surface conductance ($G_s$), (c) actual evapotranspiration ($ET$), (d) ratio between actual evapotranspiration and equilibrium evapotranspiration $ET/ET_{eq}$, and (e) decoupling coefficient (Ω) during the experiment period in the Caatinga (ESEC-Seridó). Blue and red shades represent wet and dry periods, respectively.

related to leaf growth and loss, respectively. Thus, a reduction in $G_s$ values was associated with the leaf senescence mechanism as a response to water scarcity, avoiding the excessive loss of water by plants and reducing $ET$ rates. However, $G_s$ peaks at the beginning of the wet season with the expansion of leaf cover. This indicates that $G_s$ increases might have been affected by the morphophysiological state at the leaf scale. By analyzing Fig. 4b one can notice that in the wet season of 2015 (heterogeneous rainfall distribution), $G_s$ behavior varied constantly and 25% of the values were under 0.97 mm $s^{-1}$, which means stomata were partially closed. The lag between environmental factors and soil water storage may be responsible for this oscillatory pattern in $G_s$, although explaining the causes of this phenomenon relies on complex interactions between environmental physical factors and the modulation of stomatal opening (Zhang et al., 2014; Bai et al., 2017). These $G_s$ variations in time may be related to the effects of soil water availability on stomatal opening and/or photosynthetic capacity.

$ET$ fluxes seasonal behavior was perfectly coupled to $G_s$ due to seasonal variations in leaf physiology and the effect of the forest floor $ET$ in periods of leaf loss. It is important to notice that it is difficult to individually analyze the effect of forest floor $ET$ and leaf physiology, mainly because even during the dry season there is still some tree cover due to the presence of semi-deciduous species. However, a diurnal lag was observed between $G_s$ and $ET$ which can be attributed to the estimation of $G_s$ itself. That is, in the early hours of morning stomata are already open (increasing $G_s$ values), but $ET$ is low due to low $VPD$ values. Throughout the day, $VPD$ increases and $ET$ increases with it, which explains why diurnal $ET$ peaks a couple of hours after $G_s$.

At the beginning of the wet season a sharp linear increase in $ET$ (and $G_s$) was noticed when leaf cover started to grow as soon as soil moisture was reestablished. The decrease in $ET$ values at the end of the wet season and during the wet-dry transition occurred mainly due to the reduction in stomatal opening as a defense mechanism against water stress, since diffusive resistance to water vapor reduces transpiration (Flexas et al., 2006). It is important to highlight that photosynthesis decreases with the closing of stomata due to the reduced $CO_2$ absorption (Flexas and Medrano, 2002), which leads to leaf loss (senescence) in the Caatinga under water stress conditions. Thus, low $ET$ values during the dry season can be related to the decrease in NDVI and LAI—which represents leaf senescence in the Caatinga—as a mechanism of resilience to drought, to low rainfall periods and to low

**Table 4**
Seasonal and annual total evapotranspiration in the Caatinga (total $ET$, mm) and daily means ± standard deviation for the evapotranspiration ($ET$, mm), surface conductance ($G_s$, mm $s^{-1}$), decoupling coefficient (Ω), ratio between $ET$ and equilibrium evapotranspiration ($ET/ET_{eq}$); NDVI and Leaf Area Index ($LAI$, $m^2$ $m^{-2}$).

| Variable | Dry-wet transition | | Wet season | | Wet-dry transition | | Dry season | | Annual | |
|---|---|---|---|---|---|---|---|---|---|---|
| | 2014 | 2015 | 2014 | 2015 | 2014 | 2015 | 2014 | 2015 | 2014 | 2015 |
| Total $ET$ | 87.7 | 38.6 | 307.4 | 152.6 | 53.6 | 72.7 | 24.6 | 19.5 | 473.3 | 283.4 |
| $ET$ | 1.0 ± 0.7 | 0.6 ± 0.3 | 2.6 ± 1.1 | 1.7 ± 0.9 | 0.9 ± 0.4 | 0.8 ± 0.6 | 0.3 ± 0.2 | 0.2 ± 0.1 | 1.3 ± 1.2 | 0.8 ± 0.8 |
| $G_s$ | 0.85 ± 0.83 | 0.50 ± 0.36 | 3.74 ± 2.19 | 2.13 ± 1.49 | 1.00 ± 0.65 | 0.87 ± 0.67 | 0.22 ± 0.21 | 0.13 ± 0.13 | 1.66 ± 2.00 | 0.87 ± 1.13 |
| Ω | 0.08 ± 0.07 | 0.04 ± 0.03 | 0.29 ± 0.14 | 0.17 ± 0.11 | 0.09 ± 0.06 | 0.08 ± 0.06 | 0.02 ± 0.02 | 0.01 ± 0.01 | 0.14 ± 0.15 | 0.07 ± 0.09 |
| $ET/ET_{eq}$ | 0.27 ± 0.21 | 0.18 ± 0.15 | 0.72 ± 0.30 | 0.50 ± 0.27 | 0.37 ± 0.19 | 0.30 ± 0.19 | 0.09 ± 0.06 | 0.05 ± 0.04 | 0.39 ± 0.33 | 0.24 ± 0.25 |
| NDVI | 0.46 ± 0.13 | 0.35 ± 0.08 | 0.65 ± 0.11 | 0.63 ± 0.11 | 0.46 ± 0.08 | 0.50 ± 0.08 | 0.31 ± 0.03 | 0.29 ± 0.04 | 0.49 ± 0.16 | 0.44 ± 0.16 |
| LAI | 1.21 ± 0.62 | 0.78 ± 0.23 | 1.94 ± 0.63 | 1.57 ± 0.62 | 1.07 ± 0.43 | 1.09 ± 0.47 | 0.53 ± 0.16 | 0.68 ± 0.12 | 1.26 ± 0.74 | 1.02 ± 0.53 |

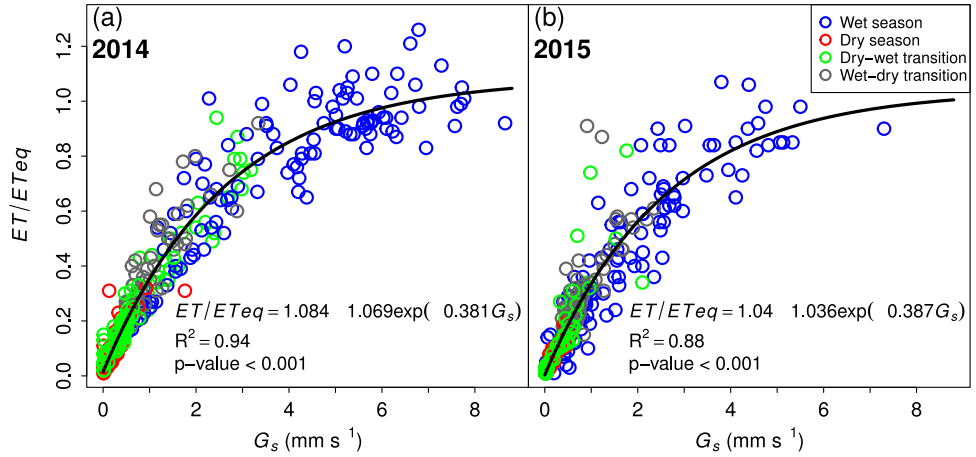


**Fig. 6.** Relationship between daily mean conductance ($G_s$) and the ratio between actual evapotranspiration and equilibrium evapotranspiration ($ET/ET_{eq}$) during 2014 (a) and 2015 (b) in the Caatinga (ESEC-Seridó)

water storage capacity of the shallow soils in the study region. Besides senescence of the leaf tissue, $G_s$ drastically reduced in the few remaining leaves of semi-deciduous species because of soil moisture deficits, which incurred in lower *ET* values. These results indicate different plant-environment interactions which affected *ET* in both study years, highlighting the role of $G_s$ in controlling evapotranspiration rates in the Caatinga according to rainfall distribution and tree cover changes.

Although 2015 was a drier year (higher atmospheric demand for water), *ET* values were lower, evidencing the highly efficient resilience mechanism of the Caatinga Biome species, which has been previously discussed and consists of stomatal closure during dry periods, reducing water lost by transpiration. This resilience can be better explained by the seasonal variations in Ω diurnal values, which will be discussed in the following sections. At the same time, the phenology of the biome promptly responds to the occurrence of rainfall, as shown by the NDVI and LAI seasonal variability (Fig. 5a), which gradually increases in the transition from the dry season to the wet season. This behavior shows that during the wet season, vegetation (mainly deciduous species) intensifies its phenological and metabolic activities (Barbosa et al., 2006; Dombroski et al., 2011; Barbosa and Kumar, 2016; da Silva et al., 2017).

Regarding *ET* behavior in the Caatinga, our results were consistent with previous studies in the semiarid region of Brazil. For example, da Silva et al. (2017) retrieved evapotranspiration in the Caatinga during 2014 and 2015 and observed higher values during the wet season and lower values during the dry season. In comparison to other forests, our results agree with the behavior observed by Ma et al. (2015) in the semiarid environment of the alpine steppes of the Tibetan Plateau, although water restrictions in this region are related to the periods of frozen soil.

Another characteristic of the Caatinga Biome which could be observed was its response to rainfall pulses with sudden increases in *ET*. A few days after the rainfall event *ET* rates exponentially decrease until they reach the rate observed before the event. Remarkable increases in *ET* after rainfall pulses were also observed by Eamus et al. (2013) during a two-year experiment in Mulga (an Australian SDTF) and by da Silva et al. (2017) in 365 days of study in a preserved Caatinga area. Furthermore, *ET* interannual patterns in the Mulga were similar to those of the present study, with daily maxima of around 3 mm day$^{-1}$ in a year with below-average and poorly distributed rainfall and daily maximums of around 4 mm day$^{-1}$ in a year with near-average homogeneously distributed rainfall. In the study conducted by da Silva et al. (2017) the wet season lasted for six months (88% of annual rainfall) and although total annual rainfall (430.2 mm year-1) was lower than in the present study, total annual *ET* (526.6 mm year-1) and maximum daily *ET* (5.4 mm year-1) were higher. These differences can probably be explained by the difference in total annual rainfall between years.

### 4.3. Analysis on the variability of the decoupling factor and $ET/ET_{eq}$

The Caatinga canopy was more decoupled from the atmosphere in the first hours of the morning, represented by high Ω values (Fig. 4e–f)

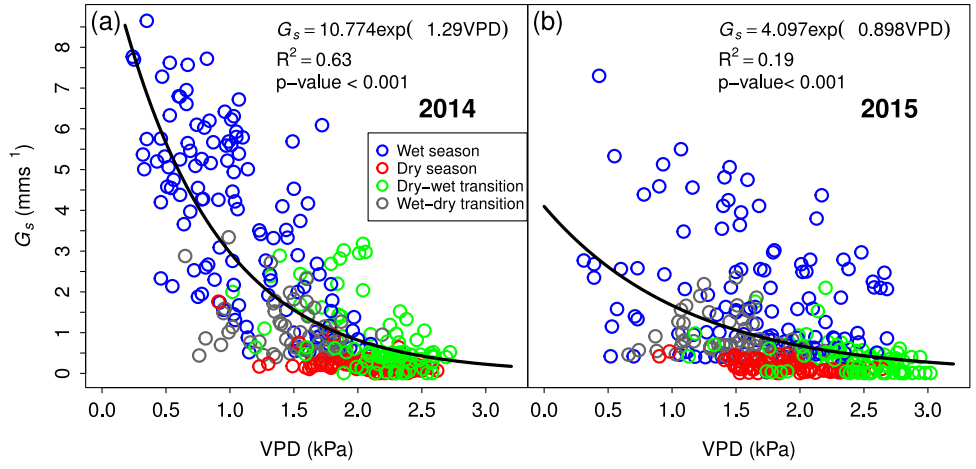


**Fig. 7.** Relationship between daily mean conductance ($G_s$) and the vapor pressure deficit (*VPD*) during 2014 (a) and 2015 (b) in the Caatinga (ESEC-Seridó)

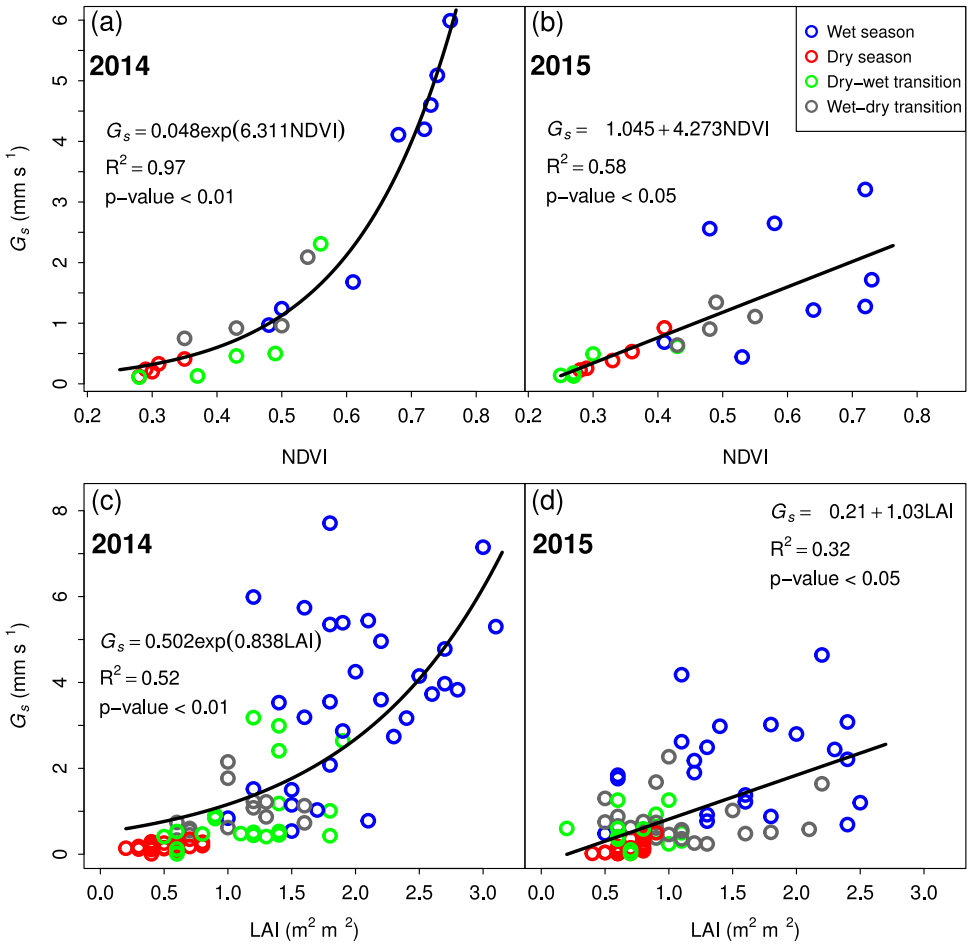


**Fig. 8.** Relationship between 16-day mean surface conductance ($G_s$) and the NDVI during 2014 (a) and 2015 (b), and between 4-day mean $G_s$ and the LAI during 2014 (c) and 2015 (d) in the Caatinga (ESEC-Seridó)

and suggesting that *ET* was controlled mainly by available energy. These high Ω values in the beginning of the morning were a consequence of high $G_s$, low *VPD* and wind speed. Throughout the day, an accentuated decrease in Ω can be observed, indicating an increasing atmosphere-canopy coupling. The explanation for the decline in Ω was the combination of the gradual decrease in $G_s$ after noon, high *VPD*, high energy availability and relatively strong winds, which usually occur during the afternoon (McNaughton and Jarvis, 1983).

The seasonal pattern of Ω was similar to that of $G_s$. Low Ω values indicated a strong control of evapotranspiration by surface conductance, particularly in the transition (wet-dry and dry-wet) and dry seasons, when Ω was lower than 0.1 (Table 4). Low Ω values are also associated with the seasonal behavior of rainfall and, consequently, with lower water availability in the soil and increasing *VPD* (Table 3). Ω values found in this study are different from the ones found by da Silva et al. (2017) in the Caatinga (average value was 0.4), although rainfall was better distributed in that study. Wever et al. (2002) also observed a decline in Ω with the reduction of soil moisture and increasing *VPD* in northern temperate grasslands during the growing season. Regarding Ω values in the wet season, the averages of 0.29 in 2014 and 0.17 in 2015 indicate that *ET* in the Caatinga was partially decoupled from the atmosphere. Considering Ω variability, one can observe that during the dry seasons, *ET* was completely controlled by the vegetation, which partially agrees with da Silva et al. (2017). Given that solar radiation is not a limiting factor for the development of the Caatinga vegetation, the decoupling is due to below-average and poorly distributed rainfall, especially in 2015.

Low $ET/ET_{eq}$ and Ω mean annual values in both years indicate that annual *ET* in the Caatinga was not limited by available energy, but by water scarcity associated with droughts. Table 5 shows a summary of rainfall and *ET* parameters in different ecosystems and in the present study. In environments with water restrictions such as the Caatinga and arid drylands, *ET* is controlled by water available in the soil, which is the main limiting factor.

### 4.4. Physiological control via surface conductance

The non-linear relationship between $ET/ET_{eq}$ and $G_s$ is consistent with studies carried out in different vegetated surfaces such as temperate deciduous forest (Wilson and Baldocchi, 2000), alpine meadows in the Tibetan Plateau (Gu et al., 2008), grasslands in the United States (Krishnan et al., 2012), corn and wheat croplands in China (Lei and Yang, 2010) and alpine steppe in the Tibetan Plateau (Ma et al., 2015).

In both years a negative physiological feedback in the canopy was observed, which agrees with the classical analysis by Jarvis and McNaughton (1986). Similar results were obtained in pastures by Wever et al. (2002), Li et al. (2005), Zhang et al. (2007), Aires et al. (2008), Ryu et al. (2008), Krishnan et al. (2012) and in forests by Granier and Bréda (1996), Zha et al. (2013) and Zhu el al. (2014). Because *ET* and $G_s$ are strongly correlated ($r \geq 0.89$ in all study period), these results are also consistent with the studies by Teixeira et al. (2008) and da Silva et al. (2017), since high *ET* values can be explained by low *VPD* which indicates an increase in the opening of stomata as a response to the water vapor transfer gradient. Fig. 7 shows that, in face of similar energy conditions, the regression curve between $G_s$ and *VPD* was better fitted in 2014 ($R^2 = 0.63$) when

**Table 5**
Comparison between accumulated rainfall (*P*), actual evapotranspiration (*ET*), daily mean latent heat flux ($\lambda E$), daily mean surface conductance ($G_s$), daily mean decoupling coefficient ($\Omega$), daily mean ratio between *ET* and equilibrium evapotranspiration ($ET_{eq}$) observed in the Caatinga and values observed in different ecosystems with similar climate characteristics.

| Vegetation type, site | Period | Total *P* (mm) | Total *ET* (mm) | Daily mean $\lambda E$ (W m$^{-2}$ day$^{-1}$)[b] | $G_s$ (mm s$^{-1}$) | $\Omega$ | $ET/ET_{eq}$ | Source |
|---|---|---|---|---|---|---|---|---|
| Caatinga SDTF, northern of Brazilian Semiarid | January 1–December 31, 2014 | 513.0 | 473.3 | 36.8 | 1.7 | 0.14 | 0.39 | In this study |
| Caatinga SDTF, northern of Brazilian Semiarid | January 1–December 31, 2015 | 466.0 | 283.4 | 22.0 | 0.9 | 0.07 | 0.24 | In this study |
| Wet temperate grassland, Japan | January 1–December 31, 1999 | 1194.2 | 808.5 | 62.8 | 11.7 | 0.65 | 1.07 | Li et al. (2005) |
| Alpine meadow grassland, Tibetan Plateau | November 11–November 10, 2002–2003 | 394.7 | 347.8 | 27.0 | 9.8 | 0.42 | 0.66 | Gu et al. (2005) |
| Alpine steppe, Tibetan Plateau | October 16–October 15, 2011–2013[a] | 337.6 | 358.2 | 27.8 | 3.5 | 0.26 | 0.35 | Ma et al. (2015) |
| Mediterranean grassland, California | January 1–April 30, 2002–2007[a] | 3366.0 | 1914 | 27.8 | 4.1 | 0.27 | 0.45 | Ryu et al. (2008) |
| Caatinga SDTF, north central of Brazilian Semiarid | March 1–February 28, 2014–2015 | 430.2 | 526.6 | 40.9 | - | 0.40 | - | da Silva et al. (2017) |

[a] Values observed in more than one study year.
[b] Daily mean $\lambda E$ values were derived from total *ET* and vice versa

compared to 2015 ($R^2$ = 0.19). In the dry season of both years *VPD* did not influence $G_s$ due to water scarcity and stomata were partially open in order to guarantee the minimum gas exchange needed for physiological and metabolic activities.

Previous studies frequently focused on the diurnal responses of $G_s$and photosynthesis, particularly their behavior observed at noon (Tucci et al., 2010; Zhang et al., 2013), which usually is exponentially or negatively related to *VPD* (Tang et al., 2006; Zhu et al., 2014; Rodrigues et al. 2016). The sensitivity of $G_s$ to changes in *VPD* was quantitatively different in each season (Fig. 7). In Fig. 7a we can clearly note a hyperbolic relationship between variables. However, this relationship occurs when there is plenty of water available, such as in 2014 when 71 rain days were registered. On the other hand, in 2015 (34 rain days) no relation between data was found (Fig. 7b). Therefore, the better fit in the hyperbolical curve adjustment is due to the effects of higher water availability on stomatal opening when *VPD* is minimum. New results were found in the present study. These different factors controlling $G_s$ according to the growth and development stage of the Caatinga plants indicate that this parameter is sensitive not only to soil water content but also to meteorological variables. This information is extremely useful in order to better understand the general behavior of stomata in response to environmental changes in different seasons.

The seasonal patterns observed in LAI is directly related to the seasonal variability of rainfall in the Caatinga, which agrees with previous studies in this biome (Barbosa et al., 2016; da Silva et al., 2017; Mutti et al., 2019) and highlights the importance of rainfall distribution to phenology, leaf growth and productivity in the Caatinga. When comparing $G_s$ versus NDVI and LAI fitted curves, one can notice that in 2014 (Fig. 8a–c) the curves were adjusted exponentially while in 2015 (Fig. 8b–d) they were linearly adjusted. This result showed that even in scenarios with limited water availability, the different temporal distribution of rainfall between the studied years resulted in different phenological responses of the plants, as evidenced by the relationships between $G_s$ and NDVI and between $G_s$ and LAI. The more evenly distributed rainfall during the year 2014 resulted in higher $G_s$ and *ET* values.

### 4.5. Comparisons with other studies

According to Table 5, daily mean $\lambda E$ values in 2014 (36.8 W m$^{-2}$) and 2015 (22.0 W m$^{-2}$) are similar to those obtained in other studies developed in ecosystems with small size vegetation (mainly grasslands) over regions with a similar climate to that of the Brazilian Semiarid region, or even in the region itself (daily mean $\lambda E$ from 27.8 to 40.9 W m$^{-2}$) (Gu et al., 2005; Ma et al., 2015, Ryu et al., 2015; da Silva et al., 2017). However, $G_s$, $\Omega$, and $ET/ET_{eq}$ values found in this study are considerably lower than values found in the aforementioned studies. These differences are possibly associated with the extreme and persistent drought condition observed during the experiment, which did not occur in said studies.

Arid and semiarid biomes cover approximately one third of the globe's surface (Lal, 2004), but a fully comprehensive understanding of the environmental factors which modulate *ET* processes and surface conductance over these regions is yet to be achieved. Therefore, there is an urgent need to investigate in detail the hydrological, atmospheric and ecological processes in SDTF. $G_s$ is a promising biophysical parameter capable of representing hydrological fluxes and their environmental controls over vegetated surfaces. Few studies have investigated the components of the energy balance and the biophysical control of evapotranspiration, but mainly over tropical humid environments and pastures.

Gu et al. (2005) observed seasonal patterns in an alpine meadow grassland and reported that vegetation phenology and soil water content were the main factors which affected energy partitioning in that ecosystem. Ma et al. (2015) quantified diurnal and seasonal *ET* variations in an alpine meadow of the Tibetan Plateau and verified that

during frozen soil and transition periods, $G_s$ values were considerably lower (0.91 and 2.45 mm $s^{-1}$, respectively), suggesting that *ET* was mainly controlled by soil moisture. In contrast, with the increase in water availability during the wet season, *ET* behavior was coupled with available energy while at the end of this season *ET* gradually decreased in response to water scarcity and plants senescence. Ryu et al. (2008) investigated *ET* interannual variability and energy exchanges in Mediterranean annual grassland, observing that *ET* was most sensitive to the availability of soil moisture during the transition to the senescence period rather than at the onset of the greenness period, causing annual evapotranspiration to be strongly modulated by growing season length.

In the Caatinga biome, da Silva et al. (2017) studied $CO_2$, water and energy fluxes and observed that in 2014 the daily mean Ω value was 28% larger than the value found in the present study and *ET* was also larger overall. However, they did not present $G_s$ values in order to investigate the biophysical controls of evapotranspiration. It should be noted that in environments with water scarcity, such as the Caatinga, *ET* is controlled by the availability of soil moisture while in humid and sub-humid tropical ecosystems available energy plays a crucial role in *ET* control, given that water is not a limiting factor. Studies using the eddy covariance method are important to better understand the behavior of stomatal modulation and its influence on the regulation of water fluxes in response to extreme environmental conditions, as suggested by Ghimire et al. (2014) and corroborated by the findings of the present study in the Caatinga Biome.

## 5. Conclusions

A seasonal analysis of the biophysical control and characteristics of *ET* was carried out in the Caatinga Biome with a detail level that is unprecedent for this biome. The physiological controls at the ecosystem level were based on surface conductance ($G_s$) and its relationships with vegetation and atmospheric parameters (NDVI, LAI and *VPD*). Additionally, we analyzed the decoupling coefficient (Ω), and the ratio between actual evapotranspiration and equilibrium evapotranspiration ($ET/ET_{eq}$). The study was conducted with data measured in a flux tower during two dry years (2014 and 2015). The present study showed that the lowest *ET* values in both years occurred in the dry season, as a consequence of leaf loss (low LAI values) or the partial closing of the stomata of the few evergreen species caused by water and rainfall shortage during this period. The highest *ET* values were registered in the wet season, when Caatinga species physiology and metabolism are fully active.

$G_s$ peaked at approximately 09:00 (local time), before *VPD* reached its maximum value. This lag between the time when $G_s$ reaches its maximum peak and the time when *VPD* reaches its maximum value is a recurring feature of forests. However, in tropical forests, which include tropical savannas, transition forests, seasonal forests and perhumid rainforests, evidences show that $G_s$ usually peaks in the early morning after sunrise.

Non-linear relationships between $G_s$ versus *VPD* and $G_s$ versus $ET/ET_{eq}$ were found, corroborating studies in other ecosystems around the world. On the other hand, the relationships between $G_s$ versus NDVI and $G_s$ versus LAI were non-linear in the year 2014 and linear in 2015. These divergences may be associated with the differences observed in total annual rainfall. The seasonal variations of $G_s$, $ET/ET_{eq}$ and Ω were remarkable, which is an expected feature of regions with a prolonged dry season (Ma et al., 2015; Tan et al., 2019). The analysis of the seasonal variation of Ω highlighted the severe drought conditions to which the region was exposed, since the surface did not decouple from the atmosphere in any day (maximum of 0.54 in the two years of this study).

Thus, results suggest that *ET* was controlled by the availability of surface water in the dry season and partially controlled by available energy during the wet season. When comparing studied years, we observed that the larger accumulated rainfall in 2014 was the most probable cause for the retrieval of higher *ET* rates in 2014 (473.3 mm) than in 2015 (283.4 mm), which incurred in lower $G_s$, decoupling coefficient (Ω) and $ET/ET_{eq}$ ratio in 2015 compared to 2014. Leaf senescence and the drastic reduction in surface conductance during the dry season allows the Caatinga Biome trees to optimize water use in order to avoid or attenuate water stress, becoming more resilient to the reduction of water availability in the soil. Major controlling factors for hydrological fluxes in this ecosystem need more attention in future researches, particularly on transpiration via sap flow monitoring.

## Declaration of Competing Interest

The authors declare that they have no known competing financial interests or personal relationships that could have appeared to influence the work reported in this paper.

## Acknowledgments

The authors are thankful to the Brazilian National Institute of Semi-Arid (INSA) and CNPq/Capes/FACEPE (Process no 465764/2014-2 and 420854/2018-5) for funding the project which originated the eddy covariance data used in this study which is partially based on the Ph.D. Thesis by Thiago Valentim Marques carried out in the Climate Sciences Graduate Program of the Federal University of Rio Grande do Norte. We are also thankful to the CNPq for funding the Research Productivity Grant to the eighth and seventeenth authors (Processes no 309165/2010-5, and 303061/2014-6, respectively) and to the ICMBio (Chico Mendes Institute for Biodiversity Conservation) for providing the experimental area and to the ESEC-Seridó (Ecological Station of Seridó) for supporting experimental activities. The authors would also like to honor Dr. Ignacio Hernán Salcedo (*in memorian*), Emeritus Professor at the Federal University of Pernambuco, former President of the INSA (2011-2015) and one of the creators of the NOWCDCB network.

## References

Aires, L.M., Pio, C.A., Pereira, J.S., 2008. The effect of drought on energy and water vapour exchange above a Mediterranean C3/C4 grassland in Southern Portugal. Agric. For. Meteorol. 148 (4), 565–579. https://doi.org/10.1016/j.agrformet.2007.11.001.

Allen, R.G., Pereira, L.S., Raes, D., Smith, M., 1998. Crop Evapotranspiration – Guidelines for Computing Crop Water Requirements - FAO Irrigation and Drainage Paper 56. Rome Italy. http://www.fao.org/docrep/X0490E/x0490e00.htm.

Althoff, T.D., Menezes, R.S.C., Carvalho, A.L., Pinto, A.S., Santiago, G.A.C.F., Ometto, J.P.H.B., Randow, S.V., Sampaio, E.V.S.B., 2016. Climate change impacts on the sustainability of the firewood harvest and vegetation and soil carbon stocks in a tropical dry forest in Santa Teresinha Municipality. Northeast Brazil. Forest Ecol. Manag. 360, 367–375. https://doi.org/10.1016/j.foreco.2015.10.001.

Alvares, C.A., Stape, J.L., Sentelhas, P.C., De Moraes Gonçalves, J.L., Sparovek, G., 2013. Köppen's climate classification map for Brazil. Meteorol. Z. 22 (6), 711–728. https://doi.org/10.1127/0941-2948/2013/0507.

Araújo, E.L., Castro, C.C., Albuquerque, U.P., 2007. Dynamics of brazilian Caatinga e a review concerning the plants, environment and people. Funct. Ecol. Comm. 1, 15–28.

Bai, B., Peviani, A., van der Horst, S., Gamm, M., Snel, B., Bentsink, L., Hanson, J., 2017. Extensive translational regulation during seed germination revealed by polysomal profiling. New Phytol 214 (1), 233–244. https://doi.org/10.1111/nph.14355.

Baldocchi, D.D., Xu, L., 2007. What limits evaporation from Mediterranean oak woodlands – the supply of moisture in the soil, physiological control by plants or the demand by the atmosphere? Adv. Water Resour 30 (10), 2113–2122. https://doi.org/10.1016/j.advwatres.2006.06.013.

Barbosa, H.A., Huete, A.R., Baethgen, W.E., 2006. A 20-year study of NDVI variability over the Northeast Region of Brazil. J. Arid Environ. 67, 288–307. https://doi.org/10.1016/j.jaridenv.2006.02.022.

Barbosa, H.A., Kumar, T.V.L., 2016. Influence of rainfall variability on the vegetation dynamics over Northeastern Brazil. J. Arid Environ. 124, 377–387. https://doi.org/10.1016/j.jaridenv.2015.08.015.

Campbell Scientific Inc, 2012. EC150 CO2 and H2O Open-path Gas Analyzer and EC100 Electronics With Optional CSAT3A 3D Sonic Anemometer. User Manual.ftp://ftp.campbellsci.com/pub/csl/outgoing/uk/manuals/ec150.pdf. (Accessed 15, December 2019).

Campos, S., Mendes, K.R., da Silva, L.L., Mutti, P.R., Medeiros, S.S., Amorim, L.B., dos Santos, C.A.C., Perez-Marin, A.M., Ramos, T.M., Marques, T.V., Lucio, P.S., Costa, G.B., Santos e Silva, C.M., Bezerra, B.G., 2019. Closure and partitioning of the energy balance in a preserved area of Brazilian seasonally dry tropical forest. Agric. For. Meteorol. 271, 398–412. https://doi.org/10.1016/j.agrformet.2019.03.018.

da Rocha, H.R., Goulden, M.L., Miler, S.D., Menton, M.C., Pinto, L.D.V.O., Freitas, H.C., Figueira, A.M.S., 2004. Seasonality of water and heat fluxes over a tropical forest in eastern Amazonia. Ecological Application 14, 22–32. https://doi.org/10.1890/02-6001.

da Silva, P.F., Lima, J.R.S., Antonino, A.C.D., Souza, R., de Souza, E.S., Silva, J.R.I., Alves, E.M., 2017. Seasonal patterns of carbon dioxide, water and energy fluxes over the Caatinga and grassland in the semi-arid region of Brazil. J. Arid Environ. 147, 71–82. https://doi.org/10.1016/j.jaridenv.2017.09.003.

Didan, K., 2015. MOD13Q1 MODIS/Terra Vegetation Indices 16-Day L3 Global 250m SIN Grid V006 [Data set]. NASA EOSDIS LP DAAC. https://doi.org/10.5067/MODIS/MOD13Q1.006.

Dombroski, J.L.D., Praxedes, S.C., de Freitas, R.M.O., Pontes, F.M., 2011. Water relations of Caatinga trees in the dry season. S. Afr. J. Bot. 77 (2), 430–434. https://doi.org/10.1016/j.sajb.2010.11.001.

Eamus, D., Cleverly, J., Boulain, N., Grant, N., Faux, R., Villalobos-Vega, R., 2013. Carbon and water fluxes in an arid-zone Acacia savanna woodland: an analyses of seasonal patterns and responses to rainfall events. Agr. For. Meteorol. 182-183, 225–238. https://doi.org/10.1016/j.agrformet.2013.04.020.

Fanourakis, D., Heuvelink, E., Carvalho, S.M.P., 2013. A comprehensive analysis of the physiological and anatomical components involved in higher water loss rates after leaf development at high humidity. J. Plant. Physiol. 170, 890–898. https://doi.org/10.1016/j.jplph.2013.01.013.

Flexas, J., Bota, J., Galmés, J., Medrano, H., Ribas-Carbo, M., 2006. Kepping a positive carbon balance under adverse conditions: responses of photosynthesis and respiration to water stress. Physiol. Plant. 127, 343–352. https://doi.org/10.1111/jac.12245.

Flexas, J., Bota, J., Loreto, F., Cornic, G., Sharkey, T.D., 2004. Diffusive and metabolic limitations to photosynthesis under drought and salinity in C3 plants. Plant Biol 6, 269–279. https://doi.org/10.1055/s-2004-820867.

Flexas, J., Medrano, H., 2002. Drought-inhibition of photosynthesis in C3 plants: stomatal and non-stomatal limitations revisited. Ann. Bot. 89 (2), 183–189. https://doi.org/10.1093/aob/mcf027.

Freitas, A.D.S., Sampaio, E.V.S.B., Santos, C.E.R.S., Fernandes, A.R., 2010. Biological nitrogen fixation in tree legumes of the Brazilian semi-arid Caatinga. J. Arid Environ. 74, 344–349. https://doi.org/10.1016/j.jaridenv.2009.09.018.

Ghimire, B., Lee, C., Heo, K., 2014. Leaf anatomy and its implications for phylogenetic relationships in Taxaceae s. l. J. Plant Res 127 (3), 373–388. https://doi.org/10.1007/s10265-014-0625-3.

Giambelluca, T.W., Scholz, F.G., Bucci, S.J., Meinzer, F.C., Goldstein, G., Hoffmann, W.A., Franco, A.C., Buchert, M.P., 2009. Evapotranspiration and energy balance of Brazilians savannas with contrasting tree density. Agric. For. Meteorol. 149, 1365–1376. https://doi.org/10.1016/j.agrformet.2009.03.006.

Gilliland, J.M., Klein, B.D, 2018. Position of the South Atlantic anticyclone and its impact on surface conditions across Brazil. J. Appl. Meteorol. Climatol. 57 (3), 535–553. https://doi.org/10.1175/JAMC-D-17-0178.1.

Granier, A., Bréda, N., 1996. Modelling canopy conductance and stand transpiration of an oak forest from sap flow measurements. Annals For. Sci. 53, 537–546. https://doi.org/10.1051/forest:19960233.

Gu, S., Tang, Y., Cui, X., Du, M., Zhao, L., Li, Y., Xu, S., Zhou, H., Kato, T., Qi, P., Zhao, X., 2008. Characterizing evapotranspiration over a meadow ecosystem on the Qinghai-Tibetan Plateau. J. Geophys. Res. 113 (D8). https://doi.org/10.1029/2007jd009173.

Gu, S., Tang, Y., Cui, X., Kato, T., Du, M., Li, Y., Zhao, X., 2005. Energy exchange between the atmosphere and a meadow ecosystem on the Qinghai-Tibetan Plateau. Agric. For. Meteorol. 129 (3–4), 175–185. https://doi.org/10.1016/j.agrformet.2004.12.002.

Hastenrath, S., 2006. Circulation and teleconnection mechanisms of Northeast Brazil droughts. Prog. Oceanogr. 70, 407–415. https://doi.org/10.1016/j.pocean.2005.07.004.

Heilman, J.L., McInnes, K., Savage, M., Gesch, R., Lascano, R.J., 1994. Soil and canopy energy balances in a west Texas vineyard. Agric. For. Meteorol. 71 (1–2), 99–114. https://doi.org/10.1016/0168-1923(94)90102-3 10.1590/0001-3765201720170206.

Igarashi, Y., Kumagai, T.O., Yoshifuji, N., Sato, T., Tanaka, N., Tanaka, K., Suzuki, M., Tantasirin, C., 2015. Environmental control of canopy stomatal conductance in a tropical deciduous forest in northern Thailand. Agric. For. Meteorol. 202, 1–10. https://doi.org/10.1016/j.agrformet.2014.11.013.

Jarvis, P.G., McNaughton, K.G., 1986. Stomatal control of transpiration: scaling up from leaf to region. Adv. Ecol. Res. 15, 1–49.

Kljun, N., Calanca, P., Rotach, M.W., Schmid, H.P., 2015. A simple two-dimensional parameterisation for Flux Footprint Prediction (FFP). Geosci. Model Dev. 8, 3695–3713. https://doi.org/10.5194/gmd-8-3695-2015.

Koch, R., Almeida-Cortez, J.S., Kleinschmit, B., 2017. Revealing areas of high nature conservation importance in a seasonally dry tropical forest in Brazil: Combination of modelled plant diversity hot spots and threat patterns. J. Nat. Conserv. 35, 24–39. https://doi.org/10.1016/j.jnc.2016.11.004.

Krishnan, P., Meyers, T.P., Scott, R.L., Kennedy, L., Heuer, M., 2012. Energy exchange and evapotranspiration over two temperate semi-arid grasslands in North America. Agric. For. Meteorol. 153, 31–44. https://doi.org/10.1016/j.agrformet.2011.09.017.

Lal, R., 2004. Soil carbon sequestration to mitigate climate change. Geoderma 123 (1–2), 1–22. https://doi.org/10.1016/j.geoderma.2004.01.032.

Leal, I.R., Silva, J.M.C., Tabarelli, M., Lacher Jr., T.E., 2005. Changing the course of biodiversity conservation the Caatinga of Northeastern Brazil. Conserv. Biol. 19 (3), 701–706. https://doi.org/10.1111/j.1523-1739.2005.00703.x.

Lei, H., Yang, D., 2010. Interannual and seasonal variability in evapotranspiration and energy partitioning over an irrigated cropland in the North China Plain. Agric. For. Meteorol. 150 (4), 581–589. https://doi.org/10.1016/j.agrformet.2010.01.022.

Li, S.G., Lai, C.T., Lee, G., Shimoda, S., Yokoyama, T., Higuchi, A., Oikawa, T., 2005. Evapotranspiration from a wet temperate grassland and its sensitivity to microenvironmental variables. Hydrol. Process. 19 (2), 517–532. https://doi.org/10.1002/hyp.5673.

Lin, Y.-S., Medlyn, B.E., Duursma, R.A., Prentice, I.C., Wang, H., Baig, S., Eamus, D., de Dios, V.R., Mitchell, P., Ellsworth, D.S., de Beeck, M.O., Wallin, G., Uddling, J., Tarvainen, L., Linderson, M.-L., Cernusak, L.A., Nippert, J.B., Ocheltree, T.W., Tissue, D.T., Martin-StPaul, N.K., Rogers, A., Warren, J.M., De Angelis, P., Hikosaka, K., Han, Q., Onoda, Y., Gimeno, T.E., Barton, C.V.M., Bennie, J., Bonal, D., Bosc, A., Löw, M., Macinins-Ng, C., Rey, A., Rowland, L., Setterfield, S.A., Tausz-Posch, S., Zaragoza-Castells, J., Broadmeadow, M.S.J., Drake, J.E., Freeman, M., Ghannoum, O., Hutley, L.B., Kelly, J.W., Kikuzawa, K., Kolari, P., Koyama, K., Limousin, J.-M., Meir, P., Lola da Costa, A.C., Mikkelsen, T.N., Salinas, N., Sun, W., Wingate, L., 2015. Optimal stomatal behaviour around the world. Nat. Clim. Change. 5, 459–464. https://doi.org/10.1038/nclimate2550.

Linares-Palomino, R., Oliveira-Filho, A.T., Pennington, R.T., 2011. Neotropical seasonally dry forests: diversity, endemism, and biogeography of woody plants. In: Dirzo, R., Young, H.S., Mooney, H.A., Ceballos, G. (Eds.), Seasonally dry tropical forests: ecology and conservation. Island Press, Washington, pp. 3–21. https://doi.org/10.5822/978-1-61091-021-7_1.

Ma, N., Zhang, Y., Guo, Y., Gao, H., Zhang, H., Wang, Y., 2015. Environmental and biophysical controls on the evapotranspiration over the highest alpine steppe. Journal of Hydrology 529, 980–992. https://doi.org/10.1016/j.jhydrol.2015.09.013.

Magrin, G.O., Marengo, J.A., Boulanger, J.-P., Buckeridge, M.S., Castellanos, E., Poveda, G., Scarano, F.R., Vicuña, S., 2014. Central and South America. In: Barros, V.R., Field, C.B., Dokken, D.J., Mastrandrea, M.D., Mach, K.J., Bilir, T.E., Chatterjee, M., Ebi, K.L., Estrada, Y.O., Genova, R.C., Girma, B., Kissel, E.S., Levy, A.N., MacCracken, S., Mastrandrea, P.R., White, L.L. (Eds.), Climate Change 2014: Impacts, Adaptation, and Vulnerability. Part B: Regional Aspects. Contribution of Working Group II to the Fifth Assessment Report of the Intergovernmental Panel on Climate Change. Cambridge University Press, Cambridge, United Kingdom, pp. 1499–1566 and New York, NY, USA.

Marengo, J.A., Alves, L.M., Alvala, R., Cunha, A.P., Brito, S., Moraes, O.L., 2017. Climatic characteristics of the 2010-2016 drought in the semiarid Northeast Brazil region. An. Acad. Bras. Cienc. 90 (2), 1973–1985.

Marengo, J.A., Bernasconi, M., 2015. Regional differences in aridity/drought conditions over Northeast Brazil: present state and future projections. Clim. Chang. 129 (1–2), 103–115. https://doi.org/10.1007/s10584-014-1310-1.

Massman, W.J., 2000. A simple method for estimating frequency response corrections for eddy covariance systems. Agric. For. Meteorol. 104, 185–198. https://doi.org/10.1016/S0168-1923(00)00164-7.

McNaughton, K.G., Jarvis, P.G., 1983. Predicting effects of vegetation changes on transpiration and evaporation. In: Kozlowski, T.T. (Ed.), Water deficits and plant growth v.7. Academic Press, New York, pp. 1–47.

Mendes, K.R., Granja, J.A.A., Ometto, J.P., Antonino, A.C.D., Menezes, R.S.C., Pereira, E.C., Pompelli, M.F., 2017. *Croton blanchetianus* modulates its morphophysiological responses to tolerate drought in a tropical dry forest. Funct. Plant Biol. 44 (10), 1039–1051. https://doi.org/10.1071/FP17098.

Miles, L., Newton, A.C., DeFries, R.S., Ravilious, C., May, I., Blyth, S., Kapos, V., Gordon, J.E., 2006. A global overview of the conservation status of tropical dry forests. J. Biogeogr. 33 (3), 491–505. https://doi.org/10.1111/j.1365-2699.2005.01424.x.

Mittermeier, R.A., Mittermeier, C.G., Brooks, T.M., Pilgrim, J.D., Konstant, W.R., da Fonseca, G.A.B., Kormos, C., 2003. Wilderness and biodiversity conservation. Proc. Natl. Acad. Sci. 100, 10309–10313. https://doi.org/10.1073/pnas.1732458100.

Monteith, J., Unsworth, M., 2013. Principles of Environmental Physics: Plants, Animals, and the Atmosphere. Elsevier, Oxford, pp. 422.

Moore, C.J., 1986. Frequency response corrections for eddy correlation systems. Boud.-Layer Meteorol. 37, 17–35.

Moura, F., de, B.P., Mendes Malhado, A.C., Ladle, R.J., 2013. Nursing the caatinga back to health. J. Arid Environ. 90, 67–68. https://doi.org/10.1016/j.jaridenv.2012.10.010.

Moura, P.M., Althoff, T.D., Oliveira, R.A., Souto, J.S., Souto, P.C., Menezes, R.S.C., Sampaio, E.V.S.B., 2016. Carbon and nutrient fluxes through litterfall at four succession stages of Caatinga dry forest in Northeastern Brazil. Nutr. Cycl. Agroecosyst. 105, 25–38. https://doi.org/10.1007/s10705-016-9771-4.

Mutti, P.R., da Silva, L.L., Medeiros, S.S., Dubreuil, V., Mendes, K.R., Marques, T.V., Lúcio, P.S., Santos e Silva, C.M., Bezerra, B.G., 2019. Basin scale rainfall-evapotranspiration dynamics in a tropical semiarid environment during dry and wet years. Int. J. Appl. Earth Obs. Geoinformation. 75, 29–43. https://doi.org/10.1016/j.jag.2018.10.007.

Myneni, R., Knyazikhin, Y., Park, T. (2015). MCD15A3H MODIS/Terra + Aqua Leaf Area Index/FPAR 4-day L4 Global 500m SIN Grid V006. NASA EOSDIS Land Processes DAAC. 10.5067/MODIS/MCD15A3H.006.

Oliveira, P.T., Santos e Silva, C.M., Lima, K.C., 2017. Climatology and trend analysis of extreme precipitation in subregions of Northeast Brazil. Theor. Appl. Climatol. 130 (1–2), 77–90. https://doi.org/10.1007/s00704-016-1865-z.

Papale, D., Reichstein, M., Aubinet, M., Canfora, E., Bernhofer, C., Kutsch, W., Longdoz, B., Rambal, S., Valentini, R., Vesala, T., Yakir, D., 2006. Towards a standardized processing of Net Ecosystem Exchange measured with eddy covariance technique: algorithms and uncertainty estimation. Biogeosciences 3, 571–583. https://doi.org/10.5194/bg-3-571-2006.

Pennington, R.T., Lewis, G.P., Ratter, J.A., 2006. An overview of the plant diversity, biogeography and conservation of neotropical savannas and seasonally dry forests. In: Pennington, R.T., Lewis, G.P., Ratter, J.A. (Eds.), Neotropical Savannas and Seasonally Dry Forests: Plant Diversity, Biogeography, and Conservation. CRC Press, Boca Raton, pp. 1–29.

Pennington, R.T., Prado, D.E., Pendry, C.A., 2000. Neotropical seasonally dry forests and Quaternary vegetation changes. J. Biogeogr. 27 (2), 261–273. https://doi.org/10.1046/j.1365-2699.2000.00397.x.

Pinho-Pessoa, A.C.B., Mendes, K.R., Jarma-Orozco, A., Pereira, M.P.S., Santos, M.A., Menezes, R.S.C., Ometto, J.P., Pereira, E.C., Pompelli, M.F., 2018. Interannual Variation in Temperature and Rainfall can Modulate the Physiological and Photoprotective Mechanisms of a Native Semiarid Plant Species. Indian J. Sci. Technol. 11 (42). https://doi.org/10.17485/ijst/2018/v11i41/130972.

Priestley, C.H.B., Taylor, R.J., 1972. On the assessment of surface heat flux and evaporation using large-scale parameters. Mon. Weather Rev. 100, 81–92. https://doi.org/10.1175/1520-0493(1972)100<0081:OTAOSH>2.3.CO;2.

R Core Team, 2018. R: a language and environment for statistical computing. In: R Foundation for Statistical Computing, Vienna, Austria. https://www.R-project.org.

Reichstein, M., Falge, E., Baldocchi, D., Papale, D., Aubinet, M., Berbigier, P., Bernhofer, C., Buchmann, N., Gilmanov, T., Granier, A., Grünwald, T., Havrankova, K., Ilvesniemi, H., Janous, D., Knohl, A., Laurila, T., Lohila, A., Loustau, D., Matteucci, G., Meyers, T., Miglietta, F., Ourcival, J.M., Pumpanen, J., Rambal, S., Rotenberg, E., Sanz, M., Tenhunen, J., Seufert, G., Vaccari, F., Vesala, T., Yakir, D., Valentini, R., 2005. On the separation of net ecosystem exchange into assimilation and ecosystem respiration: Review and improved algorithm. Glob. Chang. Biol. 11, 1424–1439. https://doi.org/10.1111/j.1365-2486.2005.001002.x.

Rodrigues, T.R., Vourlitis, G.L., Lobo, F.D.A., Oliveira, R.G., Nogueira, J.D.S., 2014. Seasonal variation in energy balance and canopy conductance for a tropical savanna ecosystem of south central Mato Grosso. Brazil. J. Geophys. Res. (Biogeoscience) 119 (1), 1–13. https://doi.org/10.1002/2013JG002472.

Rodrigues, T.R., Vourlitis, G.L., Lobo, F.D.A., Santanna, F.B., Arruda, P.H.Z.D., Nogueira, J.D.S., 2016. Modeling canopy conductance under contrasting seasonal conditions for a tropical savanna ecosystem of south central Mato Grosso. Brazil. Agric. For. Meteorol. 218–219, 218–229. https://doi.org/10.1016/j.agrformet.2015.12.060.

Ryu, Y., Baldocchi, D.D., Ma, S., Hehn, T., 2008. Interannual variability of evapotranspiration and energy exchange over an annual grassland in California. J. Geophys. Res. 113https://doi.org/10.1029/2007JD009263. D09104.

Sampaio, E.V.S.B., 1995. Overview of the Brazilian Caatinga. In: Bullock, S.H., Mooney, H.A., Medina, E. (Eds.), Seasonally Dry Tropical Forests. University Press, Cambridge, pp. 35–63.

Santana, J.A.S., Santana Júnior, J.A.S., Barreto, W.S., Ferreira, A.T.S., 2016. Estrutura e distribuição espacial da vegetação da Caatinga na Estação Ecológica do Seridó. RN. Braz. J. For. Res. 36, 355–361. https://doi.org/10.4336/2016.pfb.36.88.1002. In Portuguese.

Santos, M.G., Oliveira, M.T., Figueiredo, K.V., Falcão, H.M., Arruda, E.C.P., Almeida-Cortez, J., Sampaio, E.V.S.B., Ometto, J.P.H.B., Menezes, R.S.C., Oliveira, A.F.M., Pompelli, M.F., Antonino, A.C.D., 2014. Caatinga, the Brazilian dry tropical forest: can it tolerate climate changes? Theor. Exp. Plant Physiol. 26, 83–99. https://doi.org/10.1007/s40626-014-0008-0.

Santos, A.S., Santos e Silva, C.M., 2013. Seasonality, Interannual Variability, and Linear Tendency of Wind Speeds in the Northeast Brazil from 1986 to 2011. The Sci. World J. https://doi.org/10.1155/2013/490857. 490857.

Santos, C.A.C., Mariano, D.A., Nascimento, F.C.A., Dantas, F.R.C., Oliveira, G., Silva, M.T., Silva, L.L., Silva, B.B., Bezerra, B.G., Safa, B., Medeiros, S.S., Neale, C.M.U., 2020. Spatio-temporal patterns of energy exchange and evapotranspiration during an intense drought for drylands in Brazil. International Journal of Applied Earth Observation and Geoinformation 85, 101982. https://doi.org/10.1016/j.jag.2019.101982.

Santos, R.M., Oliveira-Filho, A.T., Eisenlohr, P.V., Queiroz, L.P., Cardoso, D.B., Rodal, M.J., 2012. Identity and relationships of the Arboreal Caatinga among other floristic units of seasonally dry tropical forests (SDTFs) of north-eastern and Central Brazil. Ecol. Evol. 2 (2), 409–428. https://doi.org/10.1002/ece3.91.

Särkinen, T., Iganci, J.R.V., Linares-Palomino, R., Simon, M.F., Prado, D.E., 2011. Forgotten forests - issues and prospects in biome mapping using Seasonally Dry Tropical Forests as a case study. BMC Ecol. 11–27. https://doi.org/10.1186/1472-6785-11-27.

Souza, L.Q., Freitas, A.D.S., Sampaio, E.V.D.S.B., Moura, P.M., Menezes, R.S.C., 2012. How much nitrogen is fixed by biological symbiosis in tropical dry forests? 1. Trees and shrubs. Nutr. Cycl. Agroecosyst 2 (94), 171–179. https://doi.org/10.1007/s10705-012-9531-z.

Stewart, J.B., 1988. Modelling surface conductance of pine forest. Agric. For. Meteorol. 43 (1), 19–35. https://doi.org/10.1016/0168-1923(88)90003-2.

Szeicz, G., Endrödi, G., Tajchman, S., 1969. Aerodynamic and surface factors in evaporation. Water Resour. Res. 5, 380–394. https://doi.org/10.1029/WR005i002p00380.

Tan, Z-H., Zhao, J-F., Wang, G-Z., Chen, M-P., Yang, L-Y., He, C-S., Restrepo-Coupe, N., Peng, S-S., Liu, X-Y., da Rocha, H.R., Kosugi, Y., Hirano, T., Saleska, S.R., Foulden, M.L., Zeng, J., Ding, F-J., Gao, F., Song, L., 2019. Surface conductance for evapotranspiration of tropical forests: Calculations, variations, and controls. Agric. For. Meteorol. 275, 317–328. https://doi.org/10.1016/j.agrformet.2019.06.006.

Tang, J., Bolstad, P.V., Ewers, B.E., Desai, A.R., Davis, K.J., Carey, E.V., 2006. Sap flux-upscaled canopy transpiration, stomatal conductance, and water use efficiency in an old growth forest in the Great Lakes region of the United States. J. Geophys. Res. 111 (G2), 1095–1100. https://doi.org/10.1029/2005JG000083.

Tavares-Damasceno, J.P., Silveira, J.L.G.S., Câmara, T., Stedile, P.C., Macario, P., Toledo-Lima, G.S., Pichorim, M., 2017. Effect of drought on demography of Pileated Finch (Coryphospingus pileatus: Thraupidae) in northeastern Brazil. J. Arid Environ. 147, 63–70. https://doi.org/10.1016/j.jaridenv.2017.09.006.

Teixeira, A.H.C., Bastiaanssen, W.G.M., Ahmad, M.D., Moura, M.S.B., Bos, M.G., 2008. Analysis of energy fluxes and vegetation-atmosphere parameters in irrigated and natural ecosystems of semi-arid Brazil. J. Hydrol. 362, 110–127. https://doi.org/10.1016/j.jhydrol.2008.08.011.

Thom, A.S., 1972. Momentum, mass and heat exchange of vegetation. Q. J. R. Meteorol. Soc. 98, 124–134. https://doi.org/10.1002/qj.49709841510.

Tomasella, J., Vieira, R.M.S.P., Barbosa, A.A., Rodriguez, D.A., Santana, M.O., Sestini, M.F., 2018. Desertification trends in the Northeast of Brazil over the period 2000–2016. Int. J. Appl. Earth. Obs. Geoinf. 73, 197–206. https://doi.org/10.1016/j.jag.2018.06.012.

Tucci, M.L.S., Erismann, N.M., Machado, E.C., Ribeiro, R.V., 2010. Diurnal and Seasonal variation in photosynthesis of peach palms grown under subtropical conditions. Photosynthetica 48 (3), 421–429. https://doi.org/10.1007/s11099-010-0055-y.

Vourlitis, G.L., Nogueira, J.S., Lobo, F.A., Sendall, K.M., Paulo, S.R., Dias, C.A.A., Pinto Jr., O.B., Andrade, N.L.R., 2008. Energy balance and canopy conductance of a tropical semi-deciduous forest of the southern Amazon Basin. Water Resour. Res. 44, W03412. https://doi.org/10.1029/2006WR005526.

Webb, E.K., Pearman, G.I., Leuning, R., 1980. Correction of flux measurements for density effects due to heat and water vapour transfer. Quart. J. Roy. Meteorol. Soc. 106, 85–100.

Wehr, R., Commane, R., Munger, J.W., McManus, J.B., Nelson, D.D., Zahniser, M.S., Saleska, S.R., Wofsy, S.C., 2017. Dynamics of canopy stomatal conductance, transpiration, and evaporation in a temperate deciduous forest, validated by carbonyl sulfide uptake. Biogeosciences 14 (2), 389–401. https://doi.org/10.5194/bg-14-389-2017.

Wever, L.A., Flanagan, L.B., Carlson, P.J., 2002. Seasonal and interannual variation in evapotranspiration, energy balance and surface conductance in a northern temperate grassland. Agric. For. Meteor. 112, 31–49. https://doi.org/10.1016/S0168-1923(02)00041-2.

Wilson, K.B., Baldocchi, D.D., 2000. Seasonal and interannual variability of energy fluxes over a broadleaved temperate deciduous forest in North America. Agric. For. Meteorol. 100 (1), 1–18. https://doi.org/10.1016/S0168-1923(99)00088-X.

Xavier, A.C., King, C.W., Scanlon, B.R., 2015. Daily gridded meteorological variables in Brazil (1980–2013). Int. J. Climatol. 36 (6), 2644–2659. https://doi.org/10.1002/joc.4518.

Zanella De Arruda, P.H., Vourlitis, G.L., Santanna, F.B., Pinto Jr., O.B., Lobo, F.A., Nogueira, J.S., 2016. Large net $CO_2$ loss from a grass-dominated tropical savanna in south-central Brazil in response to seasonal and interannual drought. J. Geophys. Res. Biogeosci. 121, 2110–2124. https://doi.org/10.1002/2016JG003404.

Zha, T., Li, C., Kellomäki, S., Peltola, H., Wang, K.Y., Zhang, Y., 2013. Controls of evapotranspiration and CO2 fluxes from scots pine by surface conductance and abiotic factors. PLoS One 8. 10.1371/journal.pone.0069027.

Zhang, Q., Manzoni, S., Katul, G., Porporato, A., Yang, D.W., 2014. The hysteretic evapotranspiration–vapor pressure deficit relation. J. Geophys. Res. Biogeo. 119 (2), 125–140. https://doi.org/10.1002/2013JG002484.

Zhang, Y., Kadota, T., Ohata, T., Oyunbaatar, D., 2007. Environmental controls on evapotranspiration from sparse grassland in Mongolia. Hydrol. Process. 21 (15), 2016–2027. https://doi.org/10.1002/hyp.6711.

Zhang, Y., Meinzer, F.C., Jin-Hua, Q., Guillermo, G., Kun-Fang, C., 2013. Midday stomatal conductance is more related to stem rather than leaf water status in subtropical deciduous and evergreen broadleaf trees. Plant Cell Environ 36 (1), 149–158. https://doi.org/10.1111/j.1365-3040.2012.02563.x.

Zhu, G., Lu, L., Su, Y., Wang, X., Cui, X., Ma, J., He, J., Zhang, K., Li, C., 2014. Energy flux partitioning and evapotranspiration in a sub-alpine spruce forest ecosystem. Hydrol. Process. 28 (19), 5093–5104. https://doi.org/10.1002/hyp.9995.